A layout design method for an industrial park based on a novel arrangement algorithm – consideration of pipe network and multiple hazard sources

Ruiqi Wang[a,b], Yufei Wang[a], Truls Gundersen[b], Yan Wu[c], Xiao Feng[c], Mengxi Liu[a]

a State Key Laboratory of Heavy Oil Processing, China University of Petroleum, Beijing, 102249, China

b Department of Energy and Process Engineering, Norwegian University of Science and Technology (NTNU), Trondheim, NO-7491, Norway

c School of Chemical Engineering and Technology, Xi'an Jiaotong University, Xi'an, Shaanxi, 710049, China

Abstract: The general layout design of an industrial park has a significant impact on safety, transportation, piping, and land occupation. Currently, the relevant studies are not mature, and most of the practical designs heavily rely on expertise. In this work, an optimization methodology is proposed to consider safety, piping connection, and occupied land simultaneously for the layout problem. A method based on an improved FLUTE algorithm is developed to optimize the pipe network arrangement. Quantitative risk analysis is employed to describe the safety aspect and the interaction among multiple hazard resources. A continuous model is used rather than a grid model to describe occupied land. The first case study illustrates that the improved FLUTE algorithm can find a better pipe network connection compared to previous algorithms with up to 38% reduction of cost. In the second case study, the layout-relevant cost from the proposed model is 6.3% lower than from a previous model, and the effectiveness of the model for multiple hazard sources is also illustrated. A Monte Carlo simulation is employed to test the optimal layout obtained from the proposed model. The results indicate the feasibility and the acceptability of accident consequences of the obtained layout. Consequently, the proposed model can significantly enhance safety and reduce capital cost for an industrial park.

Keywords: Industrial park; pipe network; layout design; FLUTE algorithm; multiple hazard sources

1 Introduction

The layout design is a critical step in the process of chemical engineering design. The cost, complexity, and safety of process operation and maintenance is highly dependent on the site location and layout. A good layout can shorten the pipes, save occupied land, enhance the inherent safety, and mitigate the Domino effect. According to statistics, 20-50 % of the total operating expenses within manufacturing is attributed to material handling, and a reasonable layout can reduce these costs by up to 10-30 %.[1]

The practical design of layouts is based on guidelines and national standards. The Center for Chemical Process Safety (CCPS) of the American Institute of Chemical Engineers (AIChE) has published a series of guidelines to enhance the safety issue in chemical engineering design[2]. However, these guidelines can only give qualitative design principles and safety suggestions for layout, and expert experience is heavily needed. Also, no optimization is applied in the practical design of layouts.

In the academic field, mathematical programming approaches are widely applied to solve industrial

layout problems. There are two types of basic models to describe industrial layout problems, i.e., grid-based models and continuous models. For grid-based models, the free space is divided equally into rectangular grids, and a facility can occupy one or more grids. Occupying one grid for each facility means ignoring facility shapes while occupying more than one grid will lead to a very complex formulation [3]. Using a grid-based model, Wang et al. [4] optimized the layout of an industrial area to improve economic performance and safety simultaneously. Martinez-Gomez et al. [5] proposed a grid-based layout model in which the units can occupy one or more grids, and the relocation of some units is allowed. As for the continuous model, the coordinates of units can vary continuously. This makes the continuous model hard to solve but more practical. Medina-Herrera et al. [6] proposed a continuous model to optimize the layout of a plant with a bowtie analysis to recognize potential catastrophic accidents. Our work is based on the continuous model.

For industrial layout problems, there are two problem scales, i.e., to determine the locations of facilities within a plant, and to determine the locations of plants in an industrial park. Most studies focus on the former one. Penteado and Ciric [7] proposed a mixed integer nonlinear programming (MINLP) model to design a safe layout for a process plant of ethylene oxide including 7 facilities. The objective function is composed of piping cost, land cost, protection devices cost, and financial risk. Their work is relatively early and comprehensive in the research field of industrial layout design. Other factors like the domino effect [8], environmental influence [9], uncertainty [10], operating conditions [11], and geographical conditions [3] are emphasized in different works. However, very few published studies focus on problems at the park level, in which the description of safety is quite different from problems at the facility level, and the piping connection becomes a major issue due to the long distances between plants. Xu et al. [12] optimized the layout of an industrial park with a constraint on toxic gas dispersion. A method to correct infeasible situations was also applied to improve the solution. Some literature mentioned in the following also focus on the park level.

In terms of safety, innumerable accidents have proved the important role of layout design in the safe operation of a factory. The explosion that occurred in BP's Texas City refinery killed 15 persons and injured more than 170 others in March 2005. One of the four critical reasons was the improper location of trailers.[13] Consequence-based quantitative risk analysis (QRA) is a common method to evaluate safety. Martinez-Gomez et al. [14] employed the TNT (Trinitrotoluene) equivalent model to estimate the consequence of Boiling Liquid Expanding Vapor Explosion (BLEVE) and to determine the facility layout. Patsiatzis et al. [15] proposed a mixed integer linear programming (MILP) model to optimize the layout based on the Dow Fire and Explosion Index (Dow F&EI). In their model, different kinds of protection devices were considered to balance economy and safety. Latifi et al. [10] considered the uncertainty of weather by processing wind data. Some other research was based on commercial safety evaluation software. Jung et al. [16] employed PHAST (ver. 6.53.1) to measure the distribution of overpressure around the process plant, and the result was further studied to obtain the risk cost. After optimization, three different layout designs were simulated using Flame Acceleration Simulator (FLACS). For the above mentioned safety-related studies, the majority was for safety evaluation in a single plant. The research on the safety of an industrial park is limited, and these studies only consider several hazard sources that do not interact with each other. In this work, the large-scale problem with multiple hazard sources is considered, and the interaction among hazard sources is analyzed on the industrial park level.

In terms of piping connections, the optimization of pipe routing was considered in some works about system integration. Alnouri et al. [17] proposed a pipe routing method to minimize the piping

cost for water integration problems, in which pipe corridors and barriers are taken into consideration. Later, the method was improved [18] to be able to merge some common pipe segments. In this way, the economic performance of the water reuse network is improved further. However, the arrangement of pipe networks, which are featured with multi-branch, like steam pipe networks, is challenging. Most research on industrial park layout neglect the arrangement of pipe networks, and only a few studies focused on it. Guirardello et al. [19] proposed an algorithm to design a pipe network with branches in 3 dimensions. However, the user needs to determine the cross points in a pipe network manually. Wu and Wang [20] first developed an approach based on the Kruskal algorithm to obtain the shortest pipe network automatically. However, the approach is extremely expensive in calculation time. In graph theory, the problem of finding the shortest connection pattern to interconnect several points with rectilinear lines is called the rectilinear Steiner minimum tree (RSMT) problem. There are many algorithms proposed for RSMT problems. Fast Lookup Table Based Wirelength Estimation (FLUTE) [21], GeoSteiner [22], and Batched Iterated 1-Steiner (BI1S) [23] are some examples of such algorithms. Some methods have been proposed based on these algorithms to design the pipe network in an industrial park. Wu et al. [24] developed a method based on the GeoSteiner software to design piecewise steam pipe networks. In their work, the mass flow rate of steam in every pipe segment are obtained by an MILP model. The FLUTE algorithm is a very fast and accurate algorithm to make an RSMT construction based on a pre-computed lookup table. In our previous work [25], an approach was developed based on the FLUTE algorithm to obtain the shortest pipe network routing. These two methods significantly reduce calculation time compared with Wu and Wang's work [20]. However, all the methods mentioned above can only find the shortest pipe network connection. Minimum length does not mean minimum cost due to the different diameters of pipe segments in the same pipe network. In this work, an improved FLUTE algorithm is proposed to identify the pipe network path with minimum cost under a certain park layout.

Industrial layout optimization problems are challenging to solve. Both Mathematical Programming approaches (often implemented and solved in GAMS - General Algebraic Modeling System) and meta-heuristic algorithms are used. Mathematical Programming approaches have shorter calculation times, but they tend to suffer from a difficulty of problem formulation and the use of gradients. Meta-heuristic methods with stochastic search for the optimum, such as Simulated Annealing and Genetic Algorithms, avoid the use of gradients, but tend to require extensive computing times. Vázquez-Román et al. [26] proposed an MINLP model to optimize a facility layout considering the potential risk of toxic release. For approaches with meta-heuristic algorithms, Caputo et al. [27] optimized the layout of facilities in a plant considering explosion scenarios based on a genetic algorithm (GA). Xie and Sahinidis [28] developed a branch-and-bound algorithm for continuous facility layout problems. Some other algorithms are also introduced to help improve solving efficiency. In the work of Wang et al. [29], the GA and a surplus rectangle fill algorithm are combined. The involvement of the surplus rectangle fill algorithm can help to exclude sparse layout designs and improve the solving efficiency. In our work, the GA is used to solve the proposed model. Therefore, compared to the existing methods, this work makes the following progresses: (1) the general layout problem for an industrial park rather than a single process is considered; (2) a continuous model is used rather than the grid-based model so that the results can be more practical; (3) a novel algorithm (improved FLUTE) is proposed to optimize the connection for pipe networks, e.g., steam pipe networks; (4) multiple hazard sources are considered so that their

interaction can be investigated. In addition, a number of comparisons and analyses is presented in this work. The novel algorithm for the pipe network arrangement is compared with a previous one in detail, as well as the corresponding layout design methods, in which the algorithms are integrated. Then the impact of multiple hazard sources on the layout is studied, and the feasibility of the proposed method is confirmed by a Monte Carlo simulation. Finally, a sensitive analysis is conducted to explore how the proposed method makes a trade-off among various aspects under different prices.

2 Problem statement

This work aims to determine the locations of plants in an industrial park considering land, piping related costs, and safety issues. The plants are treated as rectangles with different dimensions and can be rotated and arranged in any location of the industrial park to achieve an optimal layout design. The length of the pipe networks (complex pipeline with branches) and simple pipelines connecting two plants (simple pipeline without branch) are calculated based on the center points of the plants and the Manhattan distance. In this work, it is assumed that the pipelines can go through a plant and does not need to detour. Minimum length does not necessarily mean minimum cost due to the different pipe diameters in a pipe network, and it is considerably more difficult to find the most economical connection. In this work, the improved FLUTE algorithm is employed to overcome this problem.

For safety issues, the factor of multiple hazard sources of explosion accidents is considered. All plants processing explosive materials are considered potentially explosive. To implement quantitative risk analysis, a TNT equivalent model and overpressure criterion are employed to assess the consequence of an explosion. The injury to persons and damage to other plants are evaluated according to the strength of the blast wave produced by the explosion accident. The expectation of losses from explosions is considered as the risk cost, and it is integrated into the objective function. Finally, the proposed mathematical model is solved by GA to minimize the objective function.

Data provided in advance and variables to be determined are shown in the following.

Given:

- Dimensions of every plant (L_i^s , L_i^l).
- Simple connections between plants.
- Plants that should be interconnected by a pipe network.
- Unit prices of pipes with different diameters (U_m^{simple}, $U_{j,k}^{network}$).
- Mass and heat of the explosive material in every plant (M, ΔH^c).
- Number of workers in every plant (N_i).
- Investment cost of every plant ($A_i^{destroryed}$).
- Probability of explosion for each plant ($P_{i'}^{explosive}$).

Determine:

- Coordinates of the center point of every plant (x_i, y_i).
- Orientation of every plant (z_i).
- Connection patterns and the diameter of every pipe segment for pipe networks.

3 Methodology

3.1 Objective function

The objective is to minimize the total cost associated with the layout design. The total cost consists of piping cost (includes pipe network cost and simple pipeline cost), land cost, and risk cost, which can be mathematically expressed by Eq. (1).

$$\text{Min } C^{total} = C^{network} + C^{simple} + C^{land} + C^{risk} \tag{1}$$

Here, C^{total} is the total cost ($), $C^{network}$ is the capital cost of all pipe networks ($), C^{simple} is the capital cost of all simple pipelines ($), C^{land} is the land cost ($), and C^{risk} is the risk cost ($).

3.2 Pipe network cost

In this work, the pipe networks with multi-branches, for instance, steam pipe networks, are taken into account. With a pre-set constant velocity in a single pipe network, the diameters of pipes in the pipe network are different. Different diameter will result in different price per unit length. Consequently, the cost of a pipe network should be calculated piecewise according to the diameters, which can be expressed by Eq. (2).

$$C^{network} = \sum_{j \in Network} \sum_{k \in Segment_j} U_{j,k}^{segment} \times L_{j,k}^{segment} \tag{2}$$

Here, , $U_{j,k}^{segment}$ is the unit price of segment *k* in pipe network *j* ($/m), $L_{j,k}^{segment}$ is the length of pipe segment *k* in pipe network *j* (m), *Network* is the set of pipe networks, and $Segment_j$ is the set of pipe segments in pipe network *j*.

The unit price of a pipe can be obtained from the market or empirical formulas. The connection path of pipe networks and the length and diameter of every segment of a pipe network are obtained from the improved FLUTE algorithm.

3.3 Simple pipeline cost

The simple pipelines convey materials from one plant to another. The shortest length of a simple pipeline is the Manhattan distance between the two plants involved, and the cost can be obtained from Eqs. (3) and (4).

$$L_m^{simple} = \left| x_m^{outlet} - x_m^{inlet} \right| + \left| y_m^{outlet} - y_m^{inlet} \right| \quad m \in Simple \tag{3}$$

$$C^{simple} = \sum_{m \in Simple} U_m^{simple} \times L_m^{simple} \quad (4)$$

Here, $x_m^{outlet}, x_m^{inlet}, y_m^{outlet}, y_m^{inlet}$ are the coordinates of center points of the two plants connected by simple pipeline *m*, L_m^{simple} is the length of simple pipeline *m* (m), U_m^{simple} is the unit price of simple pipeline *m* ($/m), and *Simple* is the set of simple connections between plants.

3.4 Land cost

The industrial park is assumed to be a rectangle, and the proprietor should purchase the whole block of land required to place the plants. Therefore, the boundary of an industrial park and the corresponding land cost can be obtained by Eqs. (5)-(9).

$$x^{lower} = \min(x_i - \frac{L_i^x}{2}) - \frac{d}{2} \quad i \in Plant \quad (5)$$

$$x^{upper} = \max(x_i + \frac{L_i^x}{2}) + \frac{d}{2} \quad i \in Plant \quad (6)$$

$$y^{lower} = \min(y_i - \frac{L_i^y}{2}) - \frac{d}{2} \quad i \in Plant \quad (7)$$

$$y^{upper} = \max(y_i + \frac{L_i^y}{2}) + \frac{d}{2} \quad i \in Plant \quad (8)$$

$$C^{land} = (x^{upper} - x^{lower}) \times (y^{upper} - y^{lower}) \times U^{land} \quad (9)$$

Here, x^{lower}, x^{upper}, y^{lower}, and y^{upper} are the lower and upper boundary of an industrial park in the x-axis and y-axis, respectively, L_i^x and L_i^y are the side lengths of plant *i* parallel to the x-axis and the y-axis (m). U^{land} is the unit price of land ($/m^2), *d* is the minimum distance between two adjacent plants for necessary green belt and roads (m), and *Plant* is the set of plants. In this work, the boundary of the industrial park should also keep a distance from the plant nearby for the necessary green belt and roads.

3.5 Risk cost

Several plants in the area are considered to be potentially explosive, and the interaction among these hazard sources is studied. The QRA is implemented in this work to evaluate the risk and divide the area into different injury areas under a certain layout design. The expected loss from an accident is evaluated for each potentially explosive plant, and then summed up to indicate the total safety risk of the entire industrial park. The explosion is considered to occur in the center point of an explosive plant.

The TNT equivalent model is employed to evaluate the peak overpressure distribution in the industrial park when an explosion accident occurs. The overpressure of a given point in the park can be obtained from Eqs. (10)-(13) [30].

$$M^{TNT} = \alpha \frac{M\Delta H^c}{\Delta H^{TNT}} \tag{10}$$

$$F^{TNT} = \frac{R}{(M^{TNT})^{\frac{1}{3}}} \tag{11}$$

$$K^{TNT} = f_1 + f_2 \log_{10} F^{TNT} \tag{12}$$

$$\log_{10} p^o = \sum_{h=0}^{11} c_h \left(K^{TNT}\right)^h \tag{13}$$

Here, M is the mass of hydrocarbon in the plant (kg), ΔH^c is the combustion heat of hydrocarbon (kJ/kg), ΔH^{TNT} is the explosion energy of TNT (kJ/kg) which is 4190-4650 kJ/kg, α is the yield factor which is 0.03-0.04, M^{TNT} is the equivalent mass of TNT (kg), R is the distance between the receptor point and explosion center (m), F^{TNT} is the scaled distance (m/kg$^{1/3}$), K^{TNT} is an intermediate parameter, f_1, f_2, and c_h are constant parameters that are shown in Table 1, and P^0 is the peak overpressure in the receptor point (kPa).

Table 1 Parameters of the TNT equivalent model

Parameter	Value	Parameter	Value
f_1	-0.21436	f_2	1.35034
c_0	2.78077	c_1	-1.69590
c_2	-0.15416	c_3	0.51406
c_4	0.09885	c_5	-0.29391
c_6	-0.02681	c_7	0.10910
c_8	0.00163	c_9	-0.02146
c_{10}	0.00015	c_{11}	0.00168

Different peak overpressures will result in different injuries to people and buildings. Therefore, the different risk areas are defined based on peak overpressure. For buildings and facilities, the damage classification shown in Table 2[30] is used.

Table 2 Damage classification of buildings

Damage level	Peak overpressure (kPa)
Total destruction	>83
Severe damage	>35
Moderate damage	>17
Light damage	<3.5

The area where the peak overpressure is more than 83 kPa is considered as a destroyed area, and the plants completely inside the destroyed area are considered destroyed once the explosion occurs. Consequently, the loss is the purchase cost of the plant. The area with peak overpressure more than 35 kPa is considered as general damaged area, and the losses are counted as half of the purchase cost of the damaged plants. In the area with peak overpressure lower than 35 kPa, no property loss is considered due to the low repair cost. As for the plants partly covered by destroyed area and damaged area, only the covered area is accounted for in the corresponding loss.

Several plants in the industrial park are considered potentially explosive. Therefore, the property loss resulting from an explosion in Plant i' can be obtained from Eq. (14).

$$C_{i'}^{property} = \sum_{\substack{i \in Plant \\ i \neq i' \quad i,i' \in Plant}} A_i^{destroyed} \times \frac{S_{i,i'}^{destroyed}}{S_i^{full}} + \sum_{i \in Plant} A_i^{damaged} \times \frac{S_{i,i'}^{damaged}}{S_i^{full}} + A_{i'}^{destroyed} \tag{14}$$

Here, $A_i^{destroyed}$ is the purchase cost of plant *i* ($), $A_i^{damaged}$ is the repair cost of plant *i* , which is half of the purchase cost ($), $C_{i'}^{property}$ is the property loss once an explosion accident occurs in plant *e* ($), $S_{i,i'}^{destroyed}$ and $S_{i,i'}^{damaged}$ are the area of plant *i* covered by the destroyed area and damaged area of plant *e* respectively, and S_i^{full} is the full area of plant *i* The exploded plant *e* itself is considered to be destroyed completely, regardless of whether it is entirely covered by the destroyed area generated by itself (the last term in Eq. (15)). The $S_{i,i}^{destroyed}$ and $S_{i,i'}^{damaged}$ are illustrated in Figure 1.

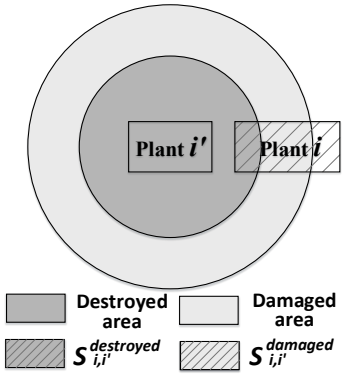

Figure 1 An illustration of $S_{i,i'}^{destroyed}$ and $S_{i,i'}^{damaged}$

For workers, the recognition of injury area is based on the possibility of eardrum rupture and death primarily from a lung hemorrhage. The probit equation relating eardrum rupture to peak overpressure is shown by Eq. (15) [30].

$$Y^{eardrum\ rupture} = -15.6 + 1.93 \ln p^o \tag{15}$$

Here, $Y^{eardrum\ rupture}$ is the probit of eardrum rupture under the overpressure of p^o.

The probit equation relating death primarily from hung hemorrhage to peak overpressure is shown by Eq. (16) [30].

$$Y^{death} = -77.1 + 6.91 \ln p^o \tag{16}$$

Here, Y^{death} is the probit of death.

The probit value can be converted into a probability with Eq. (17).

$$P = 50\left[1 + \frac{Y-5}{|Y-5|}\,\mathrm{erf}\left(\frac{Y-5}{\sqrt{2}}\right)\right] \tag{17}$$

Here, erf is the error function, *Y* is the probit and *P* is the probability of death or eardrum rupture. In this work, the area with more than 50% fatality probability is considered as death area. The area

with more than 50% eardrum rupture probability is considered as a severe injury area. The area with more than 10% probability of eardrum rupture is considered as a slight injury area. For death, severely injured, and slightly injured workers, expensive compensation is needed for them. If a plant is partly covered by injury areas, the number of casualties is also counted according to the ratio of covered area. Consequently, the casualty cost for workers can be obtained from Eq. (18).

$$C_{i'}^{people} = B^{death} \times \sum_{i \in Plant} N_i \times \frac{S_{i,i'}^{death}}{S_i^{full}} + B^{severe} \times \sum_{i \in P_{plant}} N_i \times \frac{S_{i,i'}^{severe}}{S_i^{full}} + B^{slight} \times \sum_{i \in Plant} N_i \times \frac{S_{i,i'}^{slight}}{S_i^{full}} + B^{death} \times N_{i'} \quad i \neq i' \quad i, i' \in Plant \tag{18}$$

Here, $C_{i'}^{people}$ is the total casualty cost resulting from the explosion accident of plant *i'* ($), $B^{death}, B^{severe}, B^{slight}$ are the compensations for one fatality, severely injured, and slightly injured worker, which are 1×10^7 ($/person) [10], 5×10^6 ($/person), and 1×10^6 ($/person) respectively, N_i is the number of workers in plant *i*, $S_{i,i'}^{death}, S_{i,i'}^{severe}, S_{i,i'}^{slight}$ are the areas of plant *i* covered by the death, severe, and slight injury areas of plant *e,* respectively. All the workers in the exploded plant *e* are considered to be dead (the last term in Eq. (19)).

Finally, the risk cost can be obtained by sum up the expectations of losses resulting from the explosions of plants, as is shown in Eq. (19).

$$C^{risk} = T_{life} \times \sum_{i' \in Plant} \left[(C_{i'}^{property} + C_{i'}^{people}) \times P_{i'}^{explosive} \right] \tag{19}$$

Here, $P_{i'}^{explosive}$ is the probability of explosion for plant *e*, and T_{life} is the lifetime of the park (yr).

3.6 Plant orientation

The general layout of an industrial park is in most cases organized in an orthogonal form for the convenience of design and operation. In this work, plants are allowed to rotate to obtain the optimal solution, but they can only be arranged vertically or horizontally. Therefore, a binary variable is used to indicate the orientation of a plant, as shown in Figure 2 and Eq. (20). When z_i = 1, the long edge of plant i is parallel to the x-axis; when z_i = 0 the short edge of plant i is parallel to the x-axis.

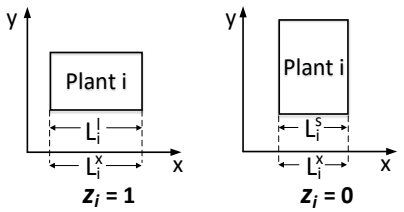

Figure 2 Diagram of plant rotation

$$L_i^x = z_i \times L_i^l + (1 - z_i) \times L_i^s \tag{20}$$

$$L_i^y = (1 - z_i) \times L_i^l + z_i \times L_i^s \tag{21}$$

Here, z_i is a binary variable indicating the orientation of plant *i*, L_i^l and L_i^s are the lengths of the long and short edges of plant *i*, respectively.

3.7 Non-overlapping constraint

Non-overlapping constraint is needed to avoid overlapping of plants. In two-dimensional space, any two plants should avoid each other in at least one dimension. A binary variable is employed to indicate the dimension in which the two plants avoid each other. The two situations should be distinguished because the non-overlapping constraint equations are different. When $w_{i,i'} = 1$, the two plants should avoid each other on the y-axis, as shown in Figure 3 (a); when $w_{i,i'} = 0$, the two plants should avoid each other on the x-axis, as shown in Figure 3 (b).

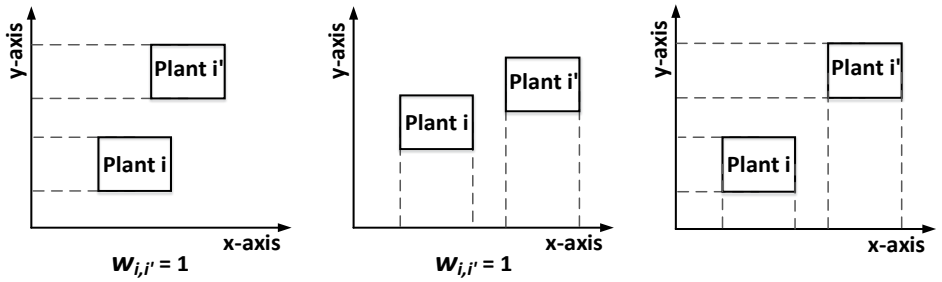

Figure 3 Illustration of the non-overlapping constraint

If two plants avoid each other in both dimensions as shown in Figure 3(c), the binary variable $w_{i,i'}$ can be either 0, or 1.

Considering minimum distance between plants, the non-overlapping constraint is expressed by Eq.(22).

$$\begin{bmatrix} w_{i,i'} \\ |y_i - y_{i'}| \geq \frac{L_i^y}{2} + \frac{L_{i'}^y}{2} + d \end{bmatrix} \vee \begin{bmatrix} 1 - w_{i,i'} \\ |x_i - x_{i'}| \geq \frac{L_i^x}{2} + \frac{L_{i'}^x}{2} + d \end{bmatrix} \quad i \neq i' \quad i, i' \in Plant \tag{22}$$

Here, $w_{i,i'}$ is a binary variable indicating the dimension in which plants *i* and *i'* avoid each other; y_i, $y_{i'}$, x_i, and $x_{i'}$ are coordinates of the two plants; *d* is the minimum distance between two adjacent plants for necessary green belt and roads.

3.8 Solution algorithm

In this work, a Genetic Algorithm is employed to solve the mathematical model proposed above. GA is a kind of stochastic algorithm, which imitates the process of biological evolution to obtain the best solution to the given mathematical model. There are three reasons for using GA: (1) GA is a common algorithm used for layout related problems, like raw material cutting problems, and has proved to be effective. (2) The improved FLUTE algorithm can only be integrated into a meta-heuristic algorithm, since gradient-based algorithms cannot be used. (3) In contrast to some other algorithms like Simulated Annealing, parallel computing technology can be applied to the GA to accelerate the solution process.

In this work, GA works as an upper-level algorithm to determine the locations of plants, while the improved FLUTE algorithm works as a lower-level algorithm to calculate pipe network cost under certain locations. The relationship between the two combined algorithms is shown in Figure 4 (a) and (b).

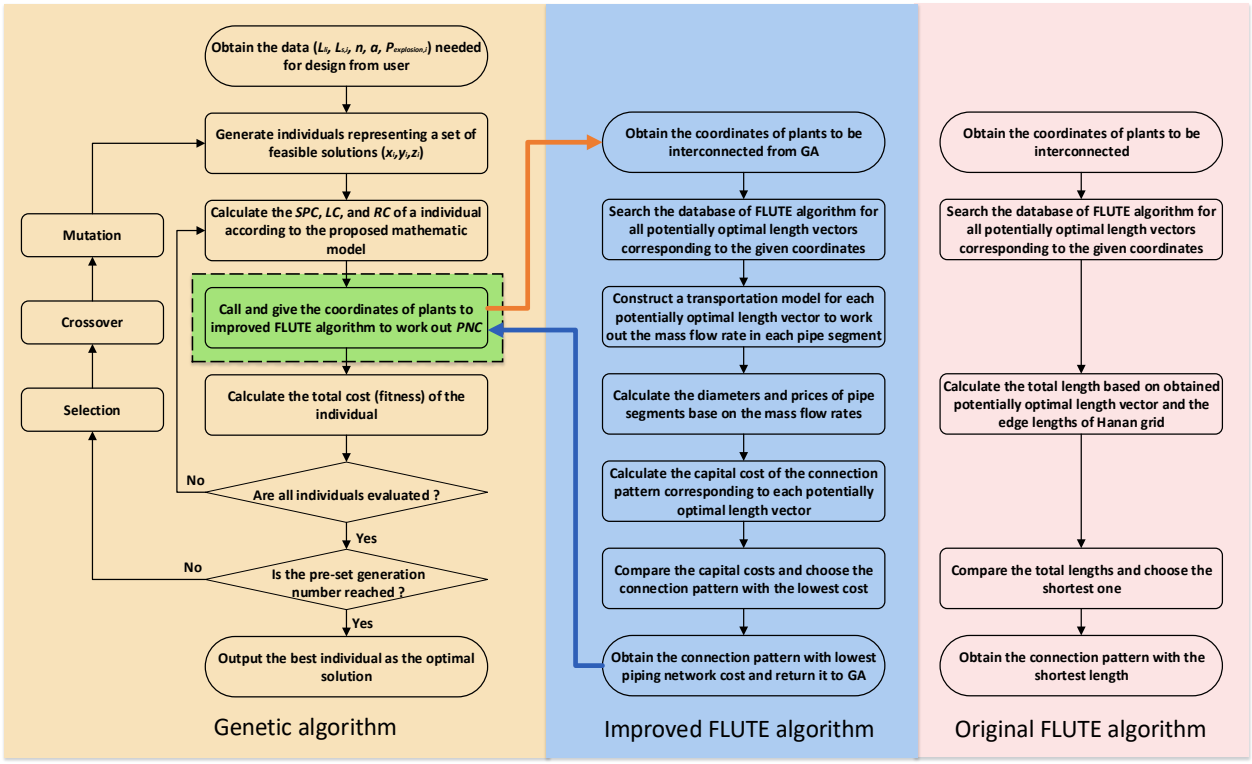

(a) (b) (c)

Figure 4 Flow diagram of algorithms

4 Improved FLUTE algorithm

Most elements in the objective function can be calculated through the description in Section 3. However, the pipe network connection with the minimum capital cost cannot be obtained. Therefore, this section is used to present the optimization algorithm for finding the most economical connection of the pipe network.

4.1 Rectilinear Steiner minimum tree problem

The problem of arranging the pipe network with the minimum capital cost is converted to a problem similar to the RSMT problem and is solved by an improved FLUTE algorithm. The original FLUTE algorithm was first developed for the RSMT problem, which is to construct a network of minimum length interconnecting a given set of points in the Euclidean plane, where each edge of the network is composed of horizontal and vertical line segments [31]. For example, the length of the connection pattern shown in Figure 5 (a) is 4, which is the minimum length to interconnect the three given points. Therefore, the connection pattern shown in Figure 5 (a) is an RSMT. In contrast, the length in Figure 5 (b) is 5, and therefore, it is not an RSMT. In this work, only the routings along

the Hanan grid is considered, because an optimal RSMT can always be constructed based on the Hanan grid [32]. The Hanan grid can be obtained by constructing horizontal and vertical lines through each given point in the plane. The dashed grid shown in Figure 5 (c) is an example of Hanan grid.

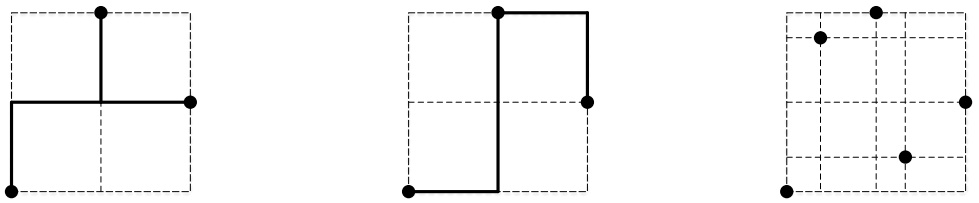

(a) (b) (c)

Figure 5 Examples of RSMT, non-RSTM and Hanan grid

4.2 Original FLUTE algorithm

The principles of the original FLUTE algorithm are briefly explained in this section for a better understanding of the improved FLUTE algorithm proposed in this work. In the original FLUTE algorithm, potentially optimal connection schemes are recorded in a database. When the coordinates of a set of points are given, the algorithm will search for and compare the potentially optimal connection schemes in the database to determine the optimal one. Some concepts and terminology should be introduced first.

Vertical sequence vector: A vertical sequence vector is used to identify sets of points with the same relative location. Such a vector can be obtained by numbering the points according to the sequence of their x-coordinates, and then sort their numbers according to their y-coordinates. For example, the vertical sequence vector of the points in Figure 6 (a) is s = (1,4,2,3). If two sets of points have the same vertical sequence vector, they have the same relative location.

Length vector: Connection schemes are stored in the form of length vectors in the database. These vectors are composed of the coefficients of the Hanan grid. For instance, the length of the connection pattern shown in Figure 6 (b) is $L_1 = h_1+2\times h_2+2\times h_3+v_1+v_2+v_3$, and the corresponding length vector is therefore p_1 = (1,2,2,1,1,1). For two connection schemes with the same vertical sequence vector, it is fairly easy to find the shorter one by length vectors. For instance, Figure 6 (c) is obviously shorter than Figure 6 (b) by comparing p_2 = (1,2,1,1,1,1) and p_1 = (1,2,2,1,1,1) directly, rather than calculating the accurate value of L_1 and L_2.

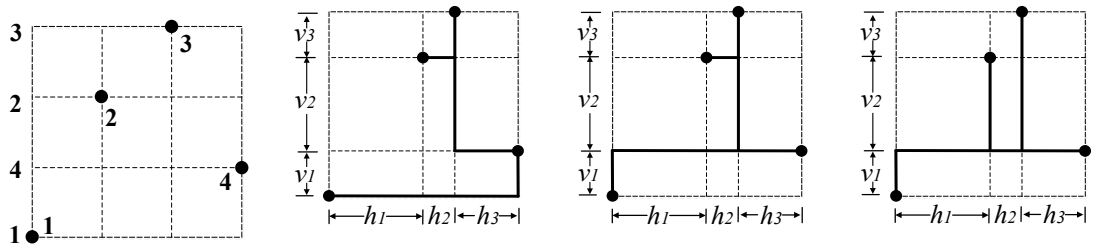

s = (1,4,2,3) p_1 = (1,2,2,1,1,1) p_2 = (1,2,1,1,1,1) p_3 = (1,1,1,1,2,1)

(a) (b) (c) (d)

Figure 6 Relative locations and three connection patterns of 4 given points

Potentially optimal length vector: The database cannot store all feasible connection schemes;

otherwise, the database will be extremely large and time consuming to search. For a vertical sequence vector, most of the feasible connection schemes can be identified to be non-optimal by comparing their length vectors. Only very few connection schemes are potentially optimal and can be pre-stored in the database. For example, the length vector of Figure 6 (d) is p_3 = (1,1,1,1,2,1), and it cannot be determined which one is the shorter of p_2 = (1,2,1,1,1,1) and p_3 = (1,1,1,1,2,1), unless the actual values of L_2 and L_3 are calculated. Both p_2 and p_3 are potentially optimal vectors if no vector is found to be shorter than them.

Therefore, when the coordinates of a set of points are given, the original FLUTE algorithm will first calculate the vertical sequence vector. The potentially optimal length vectors can then be found according to the vertical sequence vectors. The lengths of these potentially optimal length vectors are calculated and compared to determine the shortest one. The original FLUTE algorithm is extremely accurate. In a test, the average length error is only 0.075% [33]. More information about the algorithm can be found in references [21, 33-36].

4.3 Improved FLUTE algorithm

The original FLUTE algorithm can find the shortest connection pattern for a set of given points. However, for pipe networks in industrial parks, minimum length does not mean minimum cost due to the different diameters and unit prices of pipe segments. Therefore, an improved FLUTE algorithm is proposed in this work to solve this problem.

Actually, the database of the original FLUTE algorithm also contains the connection pattern with the lowest cost, which is proved in the Appendix. Therefore, the most economical connection pattern can be identified by calculating and comparing the costs of potentially optimal length vectors in the database.

The process of calculating the pipe network cost of a certain connection pattern will be explained in the following. For a certain connection pattern, a transportation model is applied to calculate the mass flow rates in different pipe segments. Wu et al. [37] obtained the flow rates in a pipe network by solving a linear programming (LP) model. Even though the LP model is fairly easy to solve, the proposed transportation model is much simpler and needs less calculations. Considering the large number of iterations in a Genetic Algorithm, this will significantly save calculation time.

In this work, a mass balance is implemented for each node to obtain the equation set of the transportation model. Here, a node represents a plant, a splitter, or a mixer. Before implementing the mass balance, the stream direction in each pipe segment should be assigned randomly, however, once the direction is determined, it cannot be changed in the mass balance for the entire pipe network. Then, a set of mass balance equations can be obtained as shown in Eq. (23).

$$\sum_{u' \in Input_t} q_{t,u'}^{inlet} - \sum_{u \in Output_t} q_{t,u}^{outlet} = Q_t \quad t \in Node \tag{23}$$

Here, Q_t is the mass flow rate demanded/produced by node t (kg/s), $q_{t,u'}^{inlet}$ is the mass flow rate of inlet stream u' to node t (kg/s), $q_{t,u}^{outlet}$ is the mass flow rate of outlet stream u from node t (kg/s), $Input_t$ is the set of streams input to node t, $Output_t$ is the set of streams output from node t, and $Node$ is the set of nodes in this network.

The mass flow rates can be obtained by solving the equation set of Eq. (23). The diameters can be

obtained by Eq. (24) with a pre-set velocity.

$$D_{j,k} = \sqrt{\frac{4 \times q_{j,k}}{\pi v_j \rho_j}} \quad j \in Network \quad k \in Segment_j \tag{24}$$

Here, $q_{j,k}$ is the mass flow rate in pipe segment k of pipe network j (kg/s), $D_{j,k}$ is the diameter of pipe segment k of pipe network j (m), v_j is the velocity of stream in pipe network j (m/s), and ρ_j is the density of the stream in pipe network j (kg/m^3).

The cost of the connection pattern corresponding to a potentially optimal length vector e can be determined by Eq. (25).

$$C_e^{potential} = \sum_{k \in Segment_e} U_{e,k}^{potential} \times L_{e,k}^{potential} \quad e \in Potential \tag{25}$$

Here, $U_{e,k}^{potential}$ is the unit price of pipe segment k which depends on $D_{j,k}$ (\$/m), $L_{e,k}^{potential}$ is the length of pipe segment k (m), $C_e^{potential}$ is the pipe network cost; all of these for the connection pattern corresponding to the potentially optimal length vector e, and *Potential* is the set of potential optimal connections for this network.

By comparing these pipe network costs ($C_e^{potential}$), the connection pattern with the lowest cost can be obtained. The flow diagrams of the improved and original FLUTE algorithms are shown in Figure 4 (b) and (c).

5 Case study

Three parts are contained in this section. In the first part, the original FLUTE algorithm is used as a representative of minimum length based algorithms to optimize the pipe network, and the improved FLUTE algorithm is employed to generate the pipe network with minimum cost. The statistic difference between the improved and original FLUTE algorithms is also studied to explore to what extent the improved FLUTE algorithm is superior to the methods aiming at minimum length. Moreover, the matching feature of the improved FLUTE algorithm in the aspect of pipe network arrangement is also explained.

In the second part, the proposed layout model is implemented in a case coming from a real petrochemical enterprise to illustrate the feasibility of the proposed model. The third part is a sensitive analysis.

5.1 Case study 1: Determining optimal pipe network connection

In this section, the improved and original FLUTE algorithms are implemented for the same case, Case A with 9 plants, to design a high-pressure steam pipe network.

The production or demand for steam and the coordinates of the 9 plants are given, as shown in Table 3. The plants are treated as points without dimension because in this case, land cost is not involved. In the table, a positive value means the plant needs steam, while a negative value means

the plant produces steam. The properties of high-pressure steam are shown in Table 4.

Table 3 The steam demands and plant coordinates of the 9 plants in Case A

Plant No.	x-axis coordinates	y-axis coordinates	Steam demand/production (D_t t/h)
1	404	908	-52
2	856	1933	42
3	1240	1391	170
4	1441	694	98
5	1034	1113	-75
6	313	1124	-87
7	1390	853	-99
8	1673	1463	-2
9	720	908	5

Table 4 The property of high-pressure steam

	Temperature T_{Tem}(℃)	Pressure p_{pre}(MPa)	Density (ρ kg/m^3)	Velocity (v m/s)
High-pressure steam	370	3.5	10.88	55

The pipe types are determined manually according to the pressure, temperature, and causticity of the material transported in the pipe. To make the calculation process simpler, only Sch 80 steel pipes are considered in this case. For detailed practical design, more pipe types should be considered according to technical conditions. The unit price (U) of a pipe depends on its diameter (D), as shown in Eqs. (26)-(29) [38].

For Sch 80 pipes:

$$U = \mathrm{E}_1 wt^{pipe} + \mathrm{E}_2 \left(D^{out} \right)^{0.48} + \mathrm{E}_3 + \mathrm{E}_4 D^{out} \tag{26}$$

$$wt^{pipe} = 1330\left(D^{inner} \right)^2 + 75.18 D^{inner} + 0.9268 \tag{27}$$

$$D^{out} = 1.101 D^{inner} + 0.006349 \tag{28}$$

$$D^{inner} = \sqrt{\frac{4q}{\pi \rho v}} \tag{29}$$

Here, U is the unit price of a pipe ($/m), E_1-E_4 are constant parameters with the values of 0.82, 185, 6.8, and 295, respectively, wt^{pipe} is the pipe weight per unit length (kg/m), D^{inner} is the inner diameter (m), D^{out} is the outer diameter (m).

The original FLUTE algorithm and the improved FLUTE algorithm are employed to design the steam pipe network and obtain the total capital cost. The program ran on a MATLAB platform and called the original and improved FLUTE algorithm written in C language. The numerical results are shown in Table 5. The connections of pipe networks are shown in Figure 7 (a) and Figure 7 (b).

Table 5 Numerical results of Case A

	Total length (m)	Total capital cost ($)	Total pipe steel weight (kg)
The Original FLUTE algorithm	3472	761,876	277,401
The Improved FLUTE algorithm	3571	698,753	234,424
Difference	2.85%	-8.29%	-15.49%

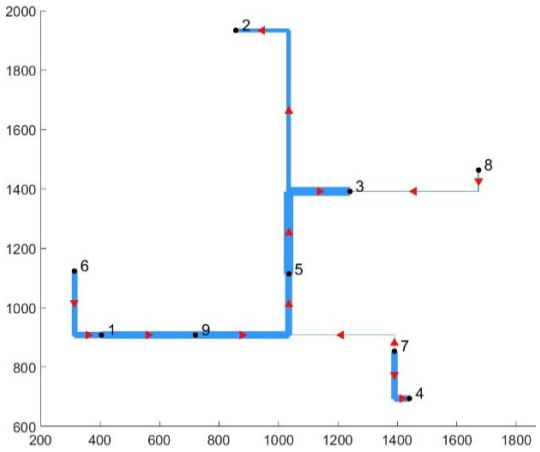

(a) Pipe network obtained from the original FLUTE algorithm

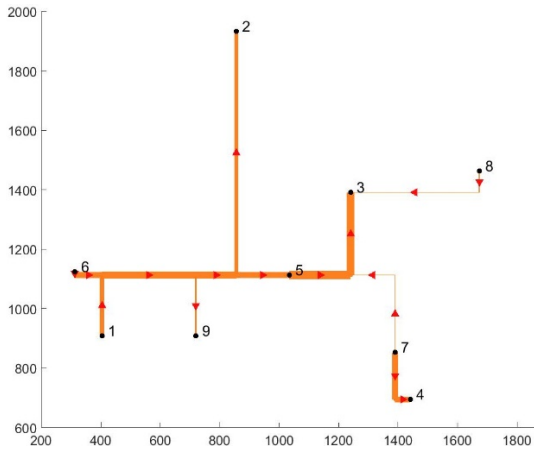

(b) Pipe network obtained from the improved FLUTE algorithm

Figure 7 Diagrams of pipe networks for Case A

In Figure 7, the widths of lines are proportional to the diameters of the pipes. The arrows indicate the flow directions of steam.

From this case, the connection patterns with minimum length and minimum cost are different. The cost of Scenario 2 is 8.29 % lower than Scenario 1. The pipe steel consumption is also significantly (15.49%) reduced. Consequently, considering the diameter is important.

5.1.1 A statistic comparison between the two types of pipe network arrangement algorithms

In the case above, the connection patterns with minimum length and minimum cost are different for the same set of points. In this section, a test is implemented to explore to what extent the improved FLUTE algorithm is more optimal than the minimum length based algorithms. The original FLUTE algorithm is employed to represent the minimum length based algorithms.

In one test, 10,000 sets of coordinates for the 9 plants are generated randomly. The demands of steam are the same as for Case A shown in Table 3. The original and the improved FLUTE algorithm are applied to design the pipe network. The costs of the 10,000 cases are recorded and processed to obtain statistics for the analysis. The test was run 5 times.

The total cost obtained from the improved FLUTE algorithm must be equal or less than that obtained from the minimum length based method. Therefore, the percentage of cost savings are used as an indicator, as shown in Eq. (30)

$$\Delta cost\ \% = \frac{C^{length} - C^{cost}}{C^{length}} \times 100\% \tag{30}$$

Here, C^{length} and C^{cost} are the costs of pipe networks obtained from the original and the improved FLUTE algorithms, respectively ($), and $\Delta cost$% is the percentage of cost saving.

Similarly, the percentage of increased length and saved steel weight for pipes are also needed, which can be obtained according to Eq. (31) and Eq. (32).

$$\Delta length\ \% = \frac{L^{cost} - L^{length}}{L^{cost}} \times 100\% \tag{31}$$

$$\Delta weight\ \% = \frac{W^{length} - W^{cost}}{W^{length}} \times 100\% \tag{32}$$

Here, L^{length} and L^{cost} are the lengths of pipe network obtained from the original and the improved FLUTE algorithms, respectively (m), W^{length} and W^{cost} are the weights of consumed pipe steel for the two obtained pipe networks (kg), Δ*length*% and Δ*weight*% are the percentage of increased length and saved weight, respectively.

Some other parameters are also needed for the statistics:

- The average percentage of cost savings and pipe steel savings of the 10,000 cases ($\overline{\Delta cost}\%$, $\overline{\Delta weight}\%$);
- The amount of cases with Δ*cost*% = 0;
- The max percentages of cost savings and pipe steel savings within the 10,000 cases (max Δ*cost*%, max Δ*weight*%);
- Calculation time for the whole test, including 10,000 cases.

The test was run 5 times on the platform of MATLAB with an i5-2310 2.9 GHz CPU and Windows 10 operating system. The improved FLUTE and original FLUTE algorithm are called by MATLAB. The statistical results are shown in Table 6.

Table 6 The statistical results of the 5 tests

Test No.	$\overline{\Delta weight}\%$	Max Δ*weight*%	$\overline{\Delta cost}\%$	Max Δ*cost*%	Number of cases with Δ*cost*%=0	Calculation time of original FLUTE algorithm (s)	Calculation time of improved FLUTE algorithm (s)
Test 1	7.72%	55.51%	3.75 %	38.18%	3721	5.77	320.76
Test 2	7.74%	50.62%	3.78%	33.99%	3696	5.88	340.81
Test 3	7.58%	50.44%	3.69%	37.95%	3776	5.73	329.98
Test 4	7.73%	49.88%	3.76%	37.60%	3778	5.75	327.58
Test 5	7.76%	52.55%	3.82%	37.05%	3738	5.60	334.35

The improved FLUTE algorithm needs more calculation time due to the increased computational load compared with the original one. Table 6 indicates that the average percentage of cost saving is approximately 3.8%. In more than one third (approximately 37%) of the conditions, the two methods will identify the same structure for the pipe network. It means, in approximately two-thirds of situations, the improved algorithm is better than the minimum length based algorithms. In the extreme case, the improved FLUTE algorithm saves up to 38% on the cost by considering piecewise diameters.

Consequently, the pipe arrangement methods aiming at minimum length are unable to identify the optimal solution in economy, while the improved FLUTE algorithm can.

Also, for Test 1, excluding the cases with the same connection patterns, the percentages of cost savings, increased length, and saved weight are counted by groups. Figure 8 (a), (b), (c) are the statistical result of Δ*cost*%, Δ*length*%, and Δ*weight*%, with a group interval of 1%, 1%, and 2%, respectively.

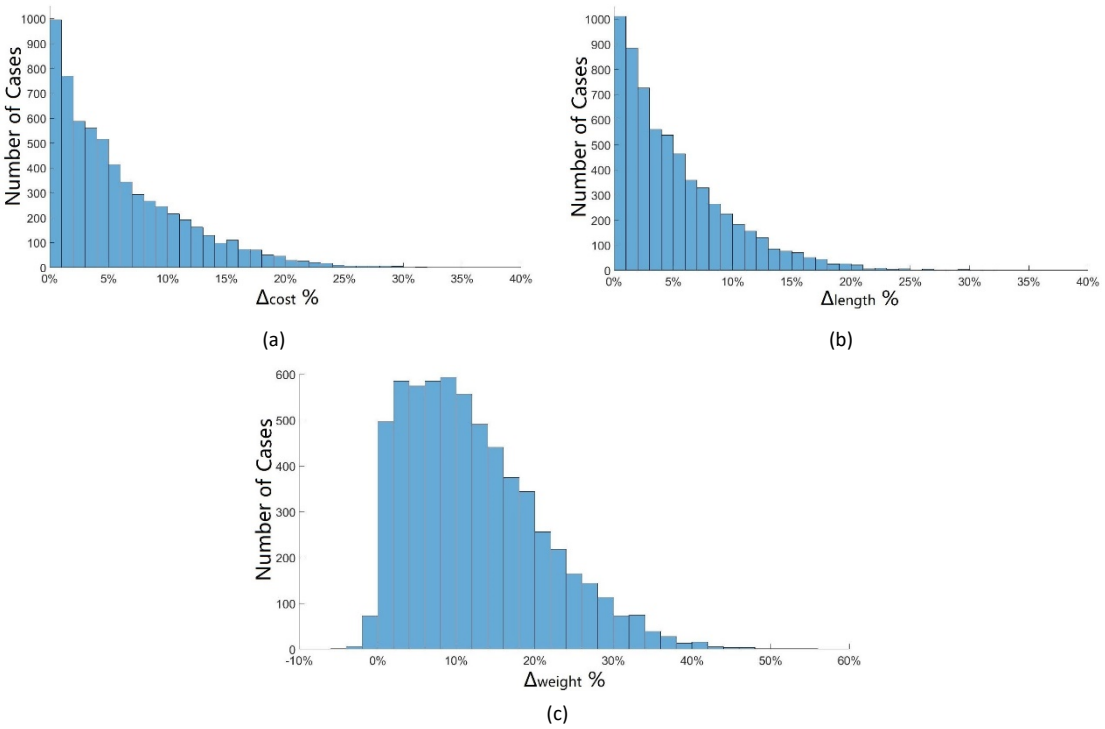

Figure 8 Diagrams with statistical results for Test 1 by grouping

In Figure 8, the distributions of Δ*cost*% and Δ*length*% are incredibly similar. However, it should be noted that the distribution groups in Figure 8 (a) and (b) are not corresponding, that is, the cases saving 10-11% cost are not always the cases increasing 10%-11% length. For instance, the case (called Case B) with the highest cost saving in Test 1 saves 38.18% cost, while the length only increases by 5.14%.From Figure 8 (c), pipe steel consumption is also reduced significantly. Interestingly, in very few cases (less than 100), pipe steel consumption is increased. Of course, this indicator depends heavily on the calculation method of pipe weight.

5.1.2 Matching feature of pipe network connections generated by the improved FLUTE algorithm

Following the statistic comparison discussed above, in this section, Case B is used to illustrate the layout feature of the improved FLUTE algorithm.

Case B comes from Test 1 and has the highest cost saving of 38.18% as well as 55.51% reduction in the consumption of pipe steel. The coordinates of plants in Case B are shown in Table 7. The numerical results are shown in Table 8. The connections are shown in Figure 9. Figure 9 (a) is from the original FLUTE algorithm, and Figure 9 (b) is from the improved algorithm. The width of a line is proportional to the diameter of the pipe.

Table 7 Coordinates of plants in Case B

Plant No.	x-coordinate	y-coordinate
1	521	499
2	830	405
3	364	1162
4	54	890

5	894	1918
6	1209	999
7	555	1759
8	1355	141
9	1272	1647

Table 8 Numerical results for Case B

	Pipe length (m)	Pipe cost ($)	Pipe steel consumption (kg)
Original FLUTE algorithm	4552	1,515,759	693,817
Improved FLUTE algorithm	4786	937,079	308,682
Difference	5.14%	-38.18%	-55.51%

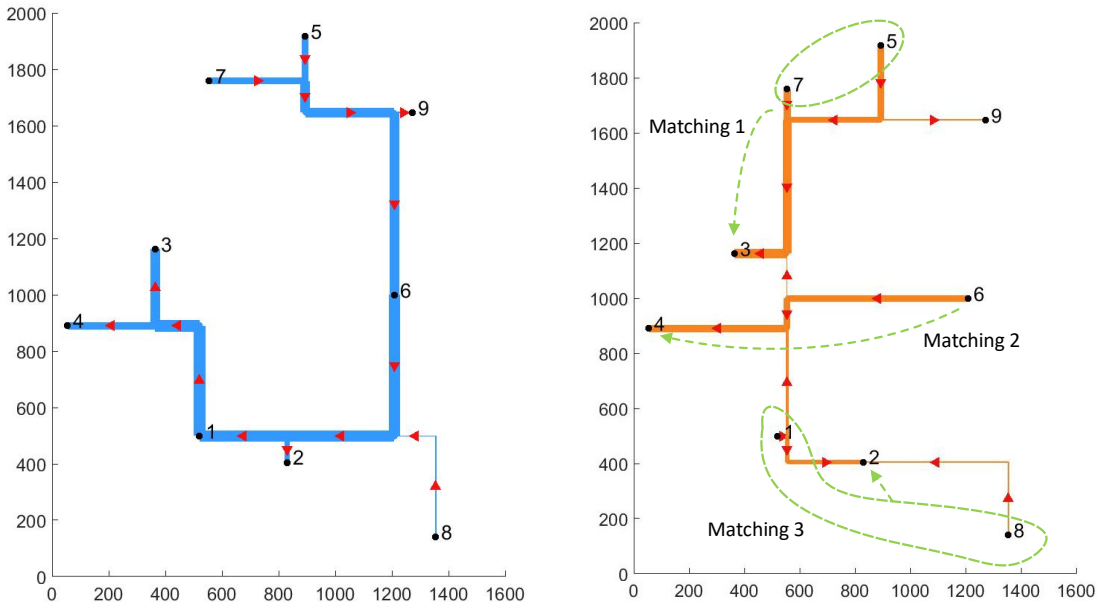

(a) Pipe network obtained from the original FLUTE algorithm (b) Pipe network obtained from the improved FLUTE algorithm

Figure 9 Diagrams of pipe networks for Case B

In Figure 9 (a), the points are connected by one main pipeline to minimize the length of pipes. The main pipeline gathers all generated steam from the producers and distributes them to consumers. However, this mode leads to heavy use of large diameter pipes and results in a high cost.

In contrast, in Figure 9 (b), the main steam producers and consumers are properly matched, and then the excess and insufficient steam are balanced by pipes with small diameters at a low price. As shown in Figure 9 (b), there are three matchings: plant 5 and 7 provide steam for plant 3; plant 6 provides steam for plant 4; plant 1 and 8 provide steam for plant 2. In each matching, steam producers and consumers are connected by pipes with smaller diameters than the main pipeline in Figure 9 (a). Therefore, the total cost is reduced.

This feature is fairly obvious in the cases with high cost savings. In cases with low cost savings, it can still be observed to a lesser degree. Due to space limitations we cannot show more cases.

Consequently, minimum length based pipe network arrangement algorithms tend to connect all plants by one main pipeline. The main pipeline will gather steam from sources and distribute to sinks. This will lead to a minimum length but heavy transportation of steam and heavy use of large diameter pipes. Additionally, the optimal connection pattern from this kind of algorithms only

depends on the coordinates of plants, while it is independent of steam demands of the plants.
The improved FLUTE algorithm (minimum cost based method) tends to match the main sources and sinks nearby to reduce the transportation of material and the use of large diameter pipes. The deficits and surplus are balanced by pipes with small diameters. This will lead to a lower total cost, but longer length compared with minimum length based algorithms. The improved algorithm can identify the main sources and sinks automatically. Therefore, the optimal connection pattern depends on both the coordinates and the steam demands of plants.

5.2 Case study 2: Determining optimal layout

In this section, the proposed layout method is implemented for a case (Case C) coming from a real petrochemical industrial park for illustration purposes. The two layout methods, integrating the original and improved FLUTE algorithm respectively, are compared.
The case contains 16 plants, and the basic data are shown in Table 9. High-pressure steam (HPS), medium-pressure steam (MPS), and low-pressure steam (LPS) are the three pipe networks considered in this case. In Table 9, a negative value for the steam demand actually means the plant produces steam. In the column of hydrocarbon mass, value 0 means the plant is not potentially explosive.
Table 9 Basic data for the plants

Plant No.	Short edge length (L_i^s m)	Long edge length (L_i^l m)	Demand for HPS (Q_t t/h)	Demand for MPS (Q_t t/h)	Demand for LPS (Q_t t/h)	Purchase cost ($C_i^{destroryed}$ ×10^3 $)	Workers (n_i)	Hydrocarbon mass (M ×10^3 kg)
1	240	300	-52	-63	0	9,700	25	0
2	130	230	42	3	-11	15,600	10	250
3	70	180	0	0	0	7,200	20	0
4	210	220	170	-9	-122	14,700	15	80
5	100	220	98	3	-47	21,600	8	100
6	90	130	0	0	0	8,200	8	0
7	70	170	-75	-25	0	18,600	10	90
8	70	170	0	0	0	9,400	10	40
9	90	220	-87	40	187	8,800	10	0
10	100	220	-99	0	18	11,400	15	40
11	110	210	-2	59	-35	17,800	10	70
12	110	210	0	0	0	15,200	12	130
13	140	240	5	-13	0	14,200	8	60
14	450	360	0	5	10	7,300	7	400
15	130	450	0	0	0	8,400	20	0
16	80	100	0	0	0	20,100	60	0

The temperature, pressure, velocity, and density of the steam types are shown in Table 10. This case also contains 32 connections (simple pipelines). The flow velocities in simple pipelines are set as 1.5 m/s for liquid materials and 30 m/s for gas materials [39]. The data of material flows in simple pipelines, and the corresponding pipe types are shown in Table 11.
Table 10 Properties of steams

	Temperature (T_{st}℃)	Pressure (p_{st} Mpa)	Density (ρ kg/m^3)	Velocity (v m/s)
High pressure steam	370	3.5	10.88	55
Medium pressure steam	250	1.1	3.90	40
Low pressure steam	160	0.4	1.68	30

Table 11 Data for material flows

Flow number	Export from Plant No.	Import to Plant No.	Mass flow rate (v_q 10^4 t/y)	Density (ρ kg/m^3)	Pipe type
1	14	2	1200	900	Sch 40
2	2	14	140	800	Sch 40
3	4	14	140	800	Sch 40
4	4	14	100	720	Sch 40
5	7	14	50	720	Sch 40
6	2	4	280	820	Sch 40
7	2	14	80	820	Sch 40
8	4	14	50	820	Sch 40
9	2	5	280	910	Sch 40
10	2	5	150	760	Sch 40
11	5	14	150	760	Sch 40
12	12	14	260	720	Sch 40
13	5	11	100	910	Sch 40
14	12	11	70	910	Sch 40
15	5	4	60	800	Sch 40
16	7	4	60	800	Sch 40
17	5	7	100	920	Sch 40
18	12	13	130	920	Sch 40
19	4	7	200	820	Sch 40
20	2	9	250	1000	Sch 80
21	8	14	45	580	Sch 40
22	9	14	50	600	Sch 80
23	10	4	0.14	0.09	Sch 80
24	10	5	0.4	0.09	Sch 80
25	10	12	0.3	0.09	Sch 80
26	3	7	5	1.2	Sch 40
27	4	7	5	1.2	Sch 40
28	3	14	10	2.02	Sch 40
29	3	14	17	1.73	Sch 40
30	7	14	20	1.73	Sch 40
31	5	10	8	1.5	Sch 40
32	4	10	25	1.5	Sch 40

In this case, both Sch 40 and Sch 80 pipes are considered. The unit price of Sch 40 pipe can be obtained from Eqs. (33)-(36).[38]

$$U = E_1 wt^{pipe} + E_2 \left(D^{out} \right)^{0.48} + E_3 + E_4 D^{out} \tag{33}$$

$$wt^{pipe} = 644.3\left(D^{inner}\right)^2 + 72.5D^{inner} + 0.4611 \tag{34}$$

$$D^{out} = 1.052D^{inner} + 0.005251 \tag{35}$$

$$D^{inner} = \sqrt{\frac{4q}{\pi\rho v}} \tag{36}$$

The minimum distance between two adjacent plants for necessary green belt and roads (d) is set to 50 m. For safety aspects, the combustion heat of hydrocarbons (ΔH^C) in a plant is determined according to the main materials contained in the plant. The energy of TNT explosion (ΔH^{TNT}) and the yield factor (α) is set to 4200 kJ/kg and 0.04. The probability of explosion accident (P) is set to 1.4×10^{-4} for every plant [30], and the lifetime is 70 years.

The model is solved by GA. The population size and generation number are set to 500 and 2000. The program ran on a workstation with two Xeon E5-2690 2.9GHz CPUs and Windows 10 operating system.

5.2.1 Optimization results

The calculation results are shown in Table 12. Scenario 1 is the layout method with the original FLUTE algorithm, while Scenario 2 is the proposed layout model with the improved FLUTE algorithm. The layout diagrams from Scenario 2 are shown in Figure 10. Figure 10 (a), (b), (c) are the connection patterns of high-, medium-, and low-pressure steam, respectively. The width of a line represents the diameter of the pipe, and the arrow indicates the flow direction of the steam. Figure 10 (d), (e), (f), (g), (h) show the injury areas.

Table 12 Calculation results for the two layout models

	Pipe network cost $C^{network}$ ($)	Simple pipeline cost C^{simple} ($)	Land cost C^{land} ($)	Risk cost C^{risk} ($)	Total cost C^{total} ($)	Pipe steel weight W (kg)	Calculation time (min)
Scenario 1	4,128,870	8,118,416	9,597,560	14,508,484	36,353,330	4,871,584	11.37
Scenario 2	3,908,967	7,047,590	8,783,550	14,305,313	34,045,420	4,397,878	66.56

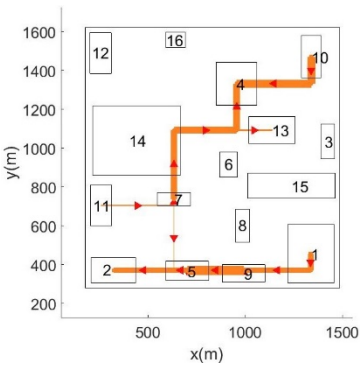

(a) High-pressure steam pipe network

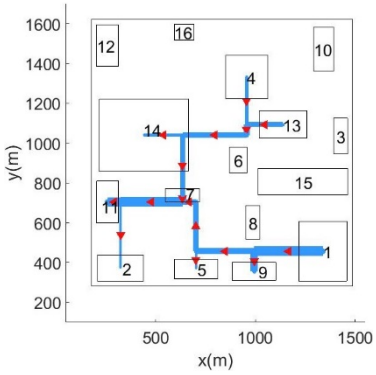

(b) Medium-pressure steam pipe network

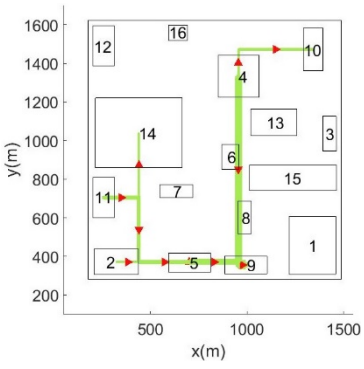

(c) Low-pressure steam pipe network

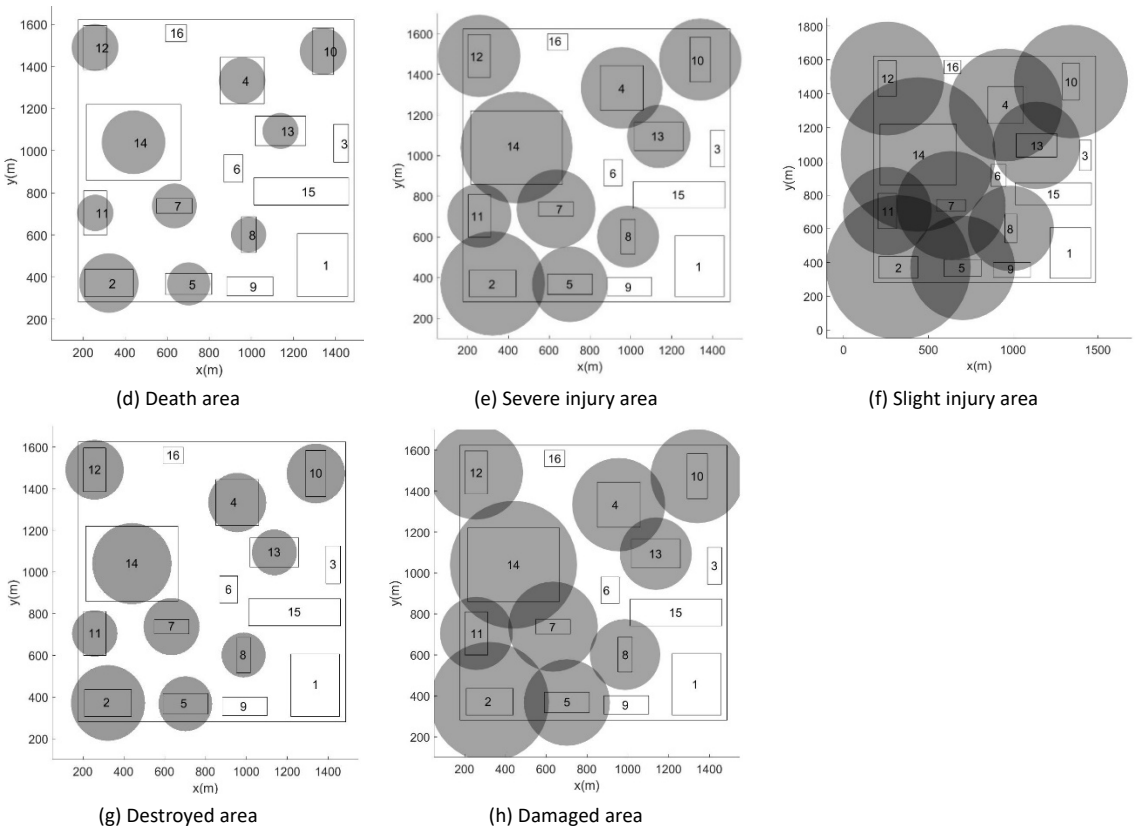

(d) Death area (e) Severe injury area (f) Slight injury area

(g) Destroyed area (h) Damaged area

Figure 10 Layout diagram for Scenario 2

From Table 12, the total cost of Scenario 2 (34,045,420 $) is 6.3% lower than Scenario 1 (36,353,330 $). With help of the improved FLUTE algorithm, the proposed layout model can find a better layout. To reduce the occupied land and pipe length, the plants should be located compactly. On the other hand, the plants should be far from each other to make the park safer. The proposed model can make a balance between the two aspects. In Figure 10, the plants are placed relatively compactly to reduce land cost and piping cost. Proper locations are also allocated to each plant to keep them safe or reduce their impact on other plants.

In Figure 10 (d), (e), (f), (g), and (h), it is worth noting that Plants 1, 3, 6, 9, and 15 are placed in the bottom right corner of the industrial park, and they are all harmless. It seems that harmless plants tend to be placed together. This phenomenon is related to safety. However, the final location of the plants is a compromise among various factors in the objective function. Therefore, this phenomenon may not be obvious in Figure 10. However, this phenomenon will be clearly demonstrated and investigated in the next section to find the reason for the behavior.

5.2.2 Discussion about the impact of multiple hazard sources

From the results obtained above, the harmless plants tend to be placed together. Safety aspects must be a reason for this phenomenon since safety is closely related to plant locations. The pipe connection may, however, influence the relative location of plants if these harmless plants have a large number of pipe connections. To explore this, the pipe related costs are removed from the objective function.

The optimization results are shown in Figure 11. Figure 11 (a), (b), (c), (d), (e) are different injury areas.

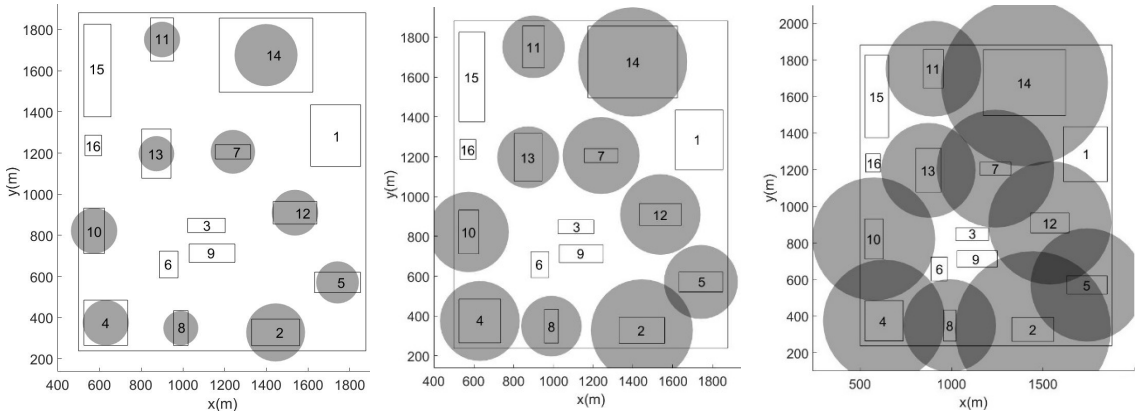

(a) Death area (b) Severe injury area (c) Slight injury area

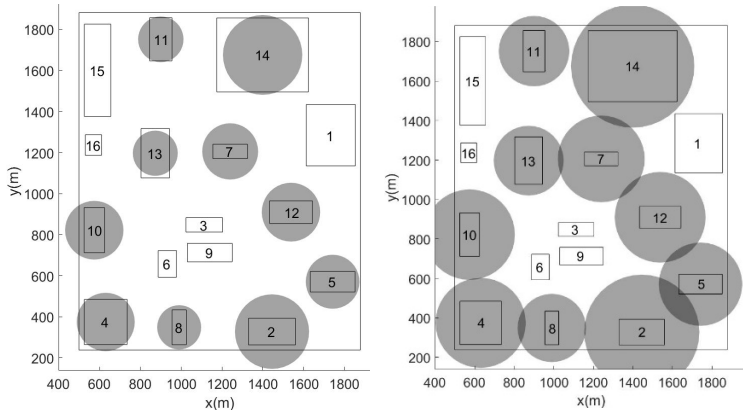

(d) Destroyed area (e) Damaged area

Figure 11 Layout diagrams from the model considering land and risk cost only

In Figure 11 (c), some harmless plants (plant 3, 6, and 9) are still placed together. The gathering area of harmless plants is exactly located in the safe area formed by slight injury areas. The gathering arrangement of harmless plants can save occupied land compared with a dispersive arrangement of harmless plants. Figure 12 (a) and (b) are a dispersive and a gathering arrangement in one-dimensional space. Obviously, the length of the gathering arrangement is shorter ($L_2<L_1$). So the gathering arrangement of harmless plants can make the layout compact under certain safety requirements.

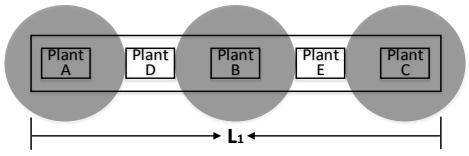

(a) Dispersive arrangement

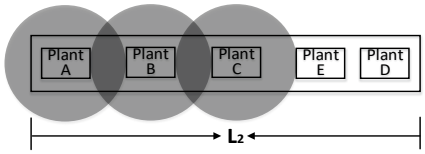

(b) Gathering arrangement

Figure 12 An illustration of dispersive and gathering arrangement

Additionally, in Figure 11, the central safe area can only accommodate a limited number of harmless plants. Other harmless plants (Plants 15, 16, and 1) are placed in the corner of the industrial park. This arrangement can make good use of the space between injury areas and park

boundary.

Consequently, the gathering effect of harmless plants emerged in Figure 10 and Figure 11 is a result of the consideration of multiple hazard sources. In this way, the occupied land can be reduced under the promise of safety.

5.2.3 Monte Carlo simulation test for the obtained layout

In the proposed model, the risk cost is calculated based on the expected financial loss of an accident. In this section, a Monte Carlo simulation is implemented to explore how many property losses and casualties there are, if the layout obtained from the proposed model in Case C is implemented.

For a virtual industrial park, each plant will every year be assessed whether to explode or not based on the probability of 1.4×10^{-4} /yr. If it explodes, the actual property loss can be found from Eqs. (10)-(14). However, for human beings, things are different. It cannot be determined which area each worker is in when an accident occurs due to the movement of workers between death area or severe injury area. Each worker will have one of the following states: death, severe injury, slight injury, or uninjured, meaning that a combination of these states in not possible. Therefore, the state of a worker is chosen randomly based on the probabilities of the four states. The probabilities can be obtained from Eqs. (37)-(40).

$$P_{i,i'}^{death} = \frac{S_{i,i'}^{death}}{S_i^{full}} \quad i,i' \in Plant \tag{37}$$

$$P_{i,i'}^{sever} = \frac{S_{i,i'}^{sever}}{S_i^{full}} \quad i,i' \in Plant \tag{38}$$

$$P_{i,i'}^{slight} = \frac{S_{i,i'}^{slight}}{S_i^{full}} \quad i,i' \in Plant \tag{39}$$

$$P_{i,i'}^{uninjured} = 1 - P_{i,i'}^{death} - P_{i,i'}^{severe} - P_{i,i'}^{slight} \quad i,i' \in Plant \tag{40}$$

Here, $P_{i,i'}^{death}, P_{i,i'}^{severe}, P_{i,i'}^{slight}, P_{i,i'}^{uninjured}$ are the probabilities of death, severe injury, slight injury, and uninjured respectively for workers in plant *i* under an explosion accident of plant *i'*.

Therefore, the annual property losses and casualties can be obtained. Figure 13 shows the process of the Monte Carlo simulation for one park within one year. The process is repeated until the park's lifetime of 70 years is reached. The simulation is implemented in 100,000 virtual industrial parks. Explosions occurred 9,808 times totally in 9,366 industrial parks. In 422 parks, the accidents occurred twice during their time life of 70 years, and three times in 10 parks. Figure 14 (a) shows the statistics of property loss, while Figure 14 (b) shows the casualties.

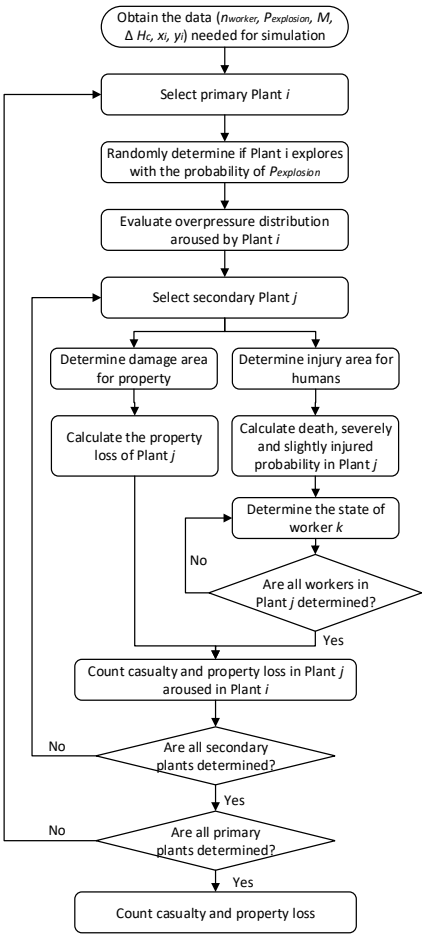

Figure 13 Flow diagram of Monte Carlo simulation

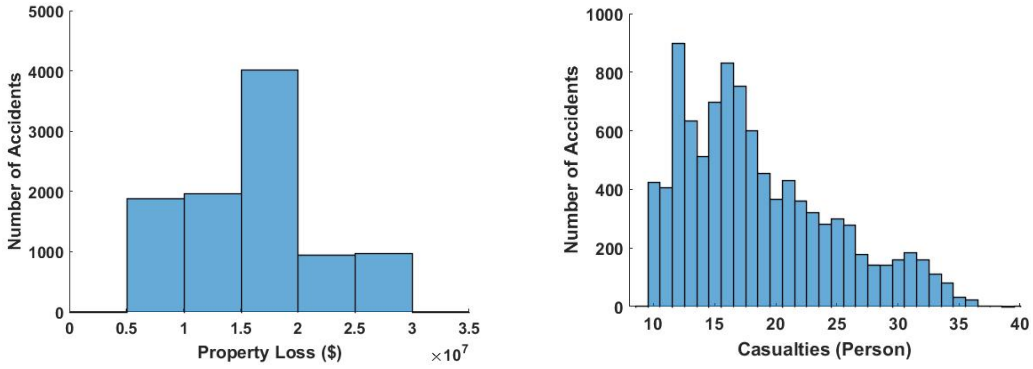

(a) (b)

Figure 14 Accident consequence statistics

Only less than 10,000 plants have explosive accidents within a period of 70 years. In most accidents, the property losses are less than 2×10^7 \$ in Figure 14 (a), and the casualties are less than 17 people in Figure 14 (b). Since the most severe condition is considered in the adopted consequence evaluation model, the accident consequences shown above are acceptable. Consequently, the layout obtained from the proposed model is feasible and practical in a real situation.

5.3 Sensitivity analysis

The land price and pipe steel price will vary in different countries and regions. The explosive

material mass is also different for plants with different process technology. In this part, sensitivity analysis is applied, and Case C is used as the base case. The piping cost, land cost, and explosive material mass are changed respectively to find the optimal layouts under different prices. The economy is not the only indicator to measure a general layout. Safety and use of natural resources should also be considered. Four indicators are calculated for the analysis: expected number of dead and severely injured workers, the expectation of property loss, occupied land area, and pipe steel weight. These four indicators refer to four aspects, i.e. personal safety, property safety, land resource, and steel resource, respectively. Additionally, the values of the 4 indicators are normalized based on the maximum value for each indicator. The maximum value within an indicator is set to 100%, and the other values are normalized based on the maximum value. In this way, we can explore how the proposed method makes a trade-off among these four aspects under various prices in different countries and regions.

5.3.1 Pipe price

The pipe prices are set to 50%, 200% and 400% of the base case respectively. The 4 indicators and normalized percentages are shown in Table 13.

Table 13 Indicator values under different pipe price

Pipe price	Expectation of death and severe injury ($\times10^{-3}$ person)	Normalized percentage	Expectation of property loss ($\times10^{3}$ \$)	Normalized percentage	Occupied land area ($\times10^{6}$ m^2)	Normalized percentage	Pipe steel consumption ($\times10^{6}$ kg)	Normalized percentage
50%	14.76	87.3%	22.08	82.0%	2.00	100.0%	4.85	100.0%
100% (Base Case)	14.95	88.4%	22.75	84.5%	1.76	88.0%	4.40	90.7%
200%	15.21	89.9%	23.42	86.9%	1.71	85.5%	3.36	69.3%
400%	16.91	100.0%	26.93	100.0%	1.63	81.5%	3.23	66.6%

From Table 13, both the pipe steel consumption and occupied land area are reduced with the increase of pipe price, while the property loss and casualties are increased. The reason is: (i) once the pipe price is increased, plants may be more compactly placed; (ii) the plants' location may be re-arranged to shorten the pipes.

For (i), besides the piping cost, it will also lead to a reduction in occupied land area. However, a short distance between plants will lead to an increase in risk. Therefore, the consumptions of pipe and land reduce, while losses of property and workers increase. For (ii), it has almost no impact on the occupied land area. Therefore, it can be noticed in Table 13 that the pipe steel consumption declines faster (100.0%→90.7%→69.3%→66.6%) than the occupied land area (100.0%→88.0%→85.5%→81.5%).

Consequently, pipe consumption is sensitive to pipe price. An increase in pipe price will lead to a more compact layout and a significant decrease in pipe consumption.

5.3.2 Land price

The land prices are set as 2, 10, and 20 \$/m^2 respectively. The 4 indicators and normalized percentages are shown in Table 14. Figure 15, Figure 16, and Figure 17 are layouts and pipe

networks under the land price of 2, 10, and 20 $/m^2 respectively. For all these figures, (a), (b), and (c) are high-, medium-, and low-pressure steam pipe networks. Figure 18 shows the slight injury area under the situation of 20 $/m^2.

Table 14 Indicator values under different land price

Land price ($/m^2)	Expectation of death and severe injury (×10^{-3} person)	Normalized percentage	Expectation of property loss (×10^3 $)	Normalized percentage	Occupied land area (×10^6 m^2)	Normalized percentage	Pipe steel consumption (×10^6 kg)	Normalized percentage
2	14.70	93.6%	21.88	94.1%	2.34	100.0%	3.84	87.3%
5 (Base Case)	14.95	95.1%	22.75	97.9%	1.76	75.2%	4.40	100.0%
10	15.71	100.0%	23.09	99.4%	1.62	69.5%	4.25	96.6%
20	15.56	99.1%	23.24	100.0%	1.54	66.0%	3.37	76.7%

In Table 14, with the increase in land price, the pipe steel consumption increased first and then reduced (87.3%→100.0%→96.6%→76.7%). The reason is that when the land price is 2 $/m^2, the plants are placed incompactly to reduce risk, and plants with steam exchanges are placed in the park center as shown in Figure 15. The major steam sources and sinks are put together, like Plant 5 and 10 in Figure 15 (a), Plant 1 and 11 in Figure 15 (b), and Plant 4, 11, and 9 in Figure 15 (c) to reduce connection cost. Plants without steam exchange are placed near the boundary, like Plant 3, 6, 8, 12, and 15. Therefore, the total pipe length is reduced compared to the base case.

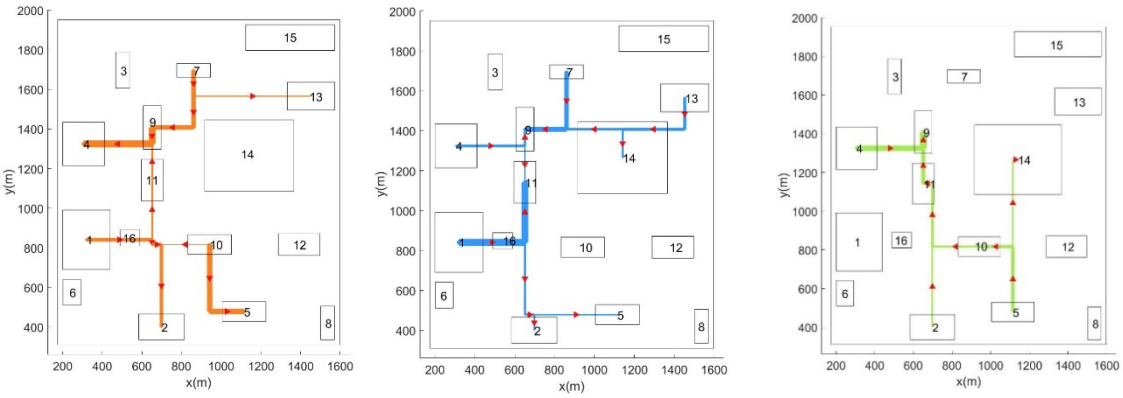

(a) High-pressure steam pipe network (b) Medium-pressure steam pipe network (c) Low-pressure steam pipe network

Figure 15 Pipe network connections with a land price of 2 $/m^2

When the land price is raised to 5 and 10 $/m^2, plants are placed more compactly to reduce occupied land area. In Table 14, the occupied land is reduced from 2.34×10^6 m^2 under the situation of 2 $/m^2 to 1.76×10^6 m^2 and 1.62×10^6 m^2 for 5 and 10 $/m^2 respectively. This will directly lead to an increase in risk. To mitigate the increase of risk and risk cost, harmless plants are put together, and each plant is allocated a proper location to ensure safety rather than to shorten the length between sources and sinks as shown in Figure 10 (d), (e), (f), (g), (h). Therefore, longer pipelines are required. As shown in Figure 10 (a), (b), (c) and Figure 16, the pipe networks spread all over the park. Therefore, in Table 14, the pipe steel consumption raised to 100.0% and 96.6% respectively under the land price of 5 and 10 $/m^2.

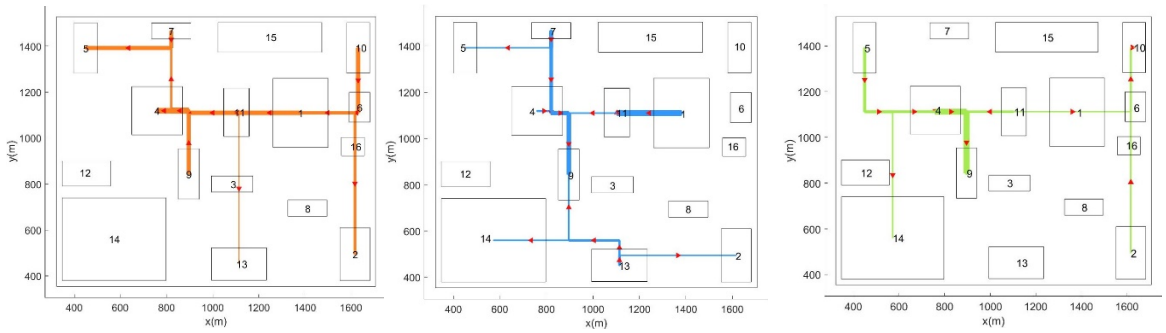

(a) High-pressure steam pipe network (b) Medium-pressure steam pipe network (c) Low-pressure steam pipe network

Figure 16 Pipe network connections with a land price of 10 $/m^2

When the land price reached 20 $/m^2, the park area is reduced further to 1.54×10^6 m^2, and as a result, almost the whole park is covered by explosive areas, as shown in Figure 18. The expectations of death and property loss also reached 99.1% and 100.0% respectively. In this condition, the gathering effect discussed in Section 5.2.2 cannot relieve the risk of the park any longer. Therefore, the main sources and sinks are placed together to shorten pipes, like Plant 10 and 5 in Figure 17 (a), Plant 1 and 11 in Figure 17 (b), and Plant 4 and 9 in Figure 17 (c). Finally, with a reduced park size and shortened pipes, pipe steel consumption is reduced to the lowest level (76.7%).

Consequently, the impact of land price on pipe consumption is fluctuating, rather than negatively correlated.

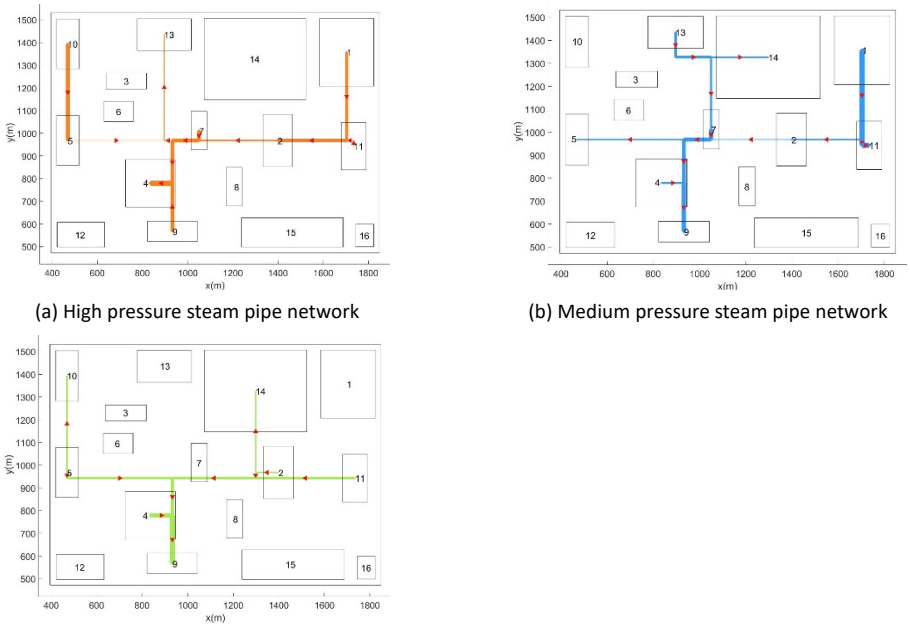

(a) High pressure steam pipe network (b) Medium pressure steam pipe network

(c) Low pressure steam pipe network

Figure 17 Pipe network connections with a land price of 20 $/m^2

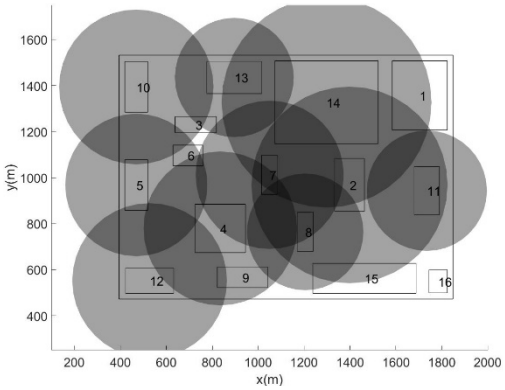

Figure 18 The slight injury areas under a land price of 20 $/m^2

5.3.3 Mass of explosive materials

The residence time and contained mass of explosive material will vary significantly with different process technologies used in a plant. Therefore, even for the plants with the same throughput and function, the amount of explosive material may still be different. The mass of explosive material is set to 50% and 200% of the base case respectively. The 4 indicators and corresponding normalized percentages are shown in Table 15.

Table 15 Indicator values under different explosive material mass

Mass of explosive material	Expectation of death and severe injury ($\times10^{-3}$ person)	Normalized percentage	Expectation of property loss ($\times10^{3}$ $)	Normalized percentage	Occupied land area ($\times10^{6}$ m^2)	Normalized percentage	Pipe steel consumption ($\times10^{6}$ kg)	Normalized percentage
50%	14.70	89.8%	21.89	88.0%	1.42	65.0%	3.57	69.1%
100% (Base Case)	14.95	91.3%	22.75	91.5%	1.76	80.7%	4.40	85.2%
200%	16.37	100.0%	24.88	100.0%	2.18	100.0%	5.16	100.0%

Obviously, more explosive material will lead to a higher risk in the park. To mitigate risk, the distances between plants are elongated. This will result in a noteworthy increase in pipe steel consumption (69.1%→85.2%→100.0%) and occupied land (65.0%→80.7%→100.0%) as shown in Table 15.

However, it is not always worthwhile to enlarge park area for safety. When the mass of explosive materials increases from 50% to 100% (Base case), the expectations of death & severe injury and property loss have almost no change (89.9% to 91.3% and 88.0% to 91.5% respectively). This indicates that the enlarged park area has basically counteracted the increased risk resulting from the increase of explosive material mass. However, when the explosive material increases from 100% to 200%, both expectations of casualties and property loss increase from about 91% to 100%. In this condition, the capital cost needed to keep the park safe is much higher than the loss resulting from the accident. It is not worthwhile to keep the park at a low-risk level. Therefore, employing proper process technology to reduce the contained explosive material in the plants is an effective way to enhance safety and reduce capital cost.

6 Conclusion

In this work, an improved FLUTE algorithm and a layout design method considering multiple hazard sources are proposed. It is important to consider diameters when designing pipe network routings. In a large-scale test, the improved FLUTE algorithm can save up to 38.18% cost comparing with a previous method. Therefore, the improved FLUTE algorithm can find a more economical pipe network connection. Also, the improved algorithm tends to match the main sources and sinks in a network to reduce the use and diameters of pipes, which is called matching feature. With the help of the improved FLUTE algorithm, the proposed layout design method can reduce total cost by 6.3% in the demonstrated case.

In terms of safety, the situation of multiple hazard sources, which is more realistic, is considered in the proposed layout design model. It is found that harmless plants tend to be placed together to reduce the risk of the park. Additionally, a Monte Carlo simulation for 100,000 virtual industrial parks shows that the property losses and casualties are less than 2×10^7 \$ and 17 people within the 70-year life-time of most parks. The simulation demonstrates the feasibility and reliability of the layout obtained from the proposed method. Finally, a sensitive analysis is implemented. The pipe steel consumption peaks when land price is about 5 - 10 \$/m^2. Therefore, the impact of land price on pipe steel consumption is fluctuating, rather than being entirely negatively correlated. Employing process technologies with less explosive materials is an effective way to enhance safety, which is also emphasized in the conception of inherent safety.

7 Acknowledgment

The author of the FLUTE algorithm, Dr. Chris C. N. Chu Iowa State University, and his FLUTE algorithm are greatly acknowledged. Financial support from , and the China Scholarship Council (No.201906440120) are also greatly acknowledged.

References:

1. Tompkins, J. A.; White, J. A.; Bozer, Y. A.; Tanchoco, J. M. A., *Facilities planning*. 4th ed.; John Wiley & Sons: New York, 2010.
2. CCPS, *Guidelines for Siting and Layout of Facilities*. 2nd ed.; John Wiley & Sons: New York, 2018.
3. Ozyurt, D. B.; Realff, M. J., Geographic and process information for chemical plant layout problems. *Journal of American Institute of Chemical Engineers* **1999,** 45, (10), 2161-2174.
4. Wang, R.; Wu, Y.; Wang, Y.; Feng, X., An industrial area layout design methodology considering piping and safety using genetic algorithm. *Journal of Cleaner Production* **2017,** 167, 23-31.
5. Martinez-Gomez, J.; Nápoles-Rivera, F.; Ponce-Ortega, J. M.; Serna-González, M.; El-Halwagi, M. M., Siting Optimization of Facility and Unit Relocation with the Simultaneous Consideration of Economic and Safety Issues. *Industrial & Engineering Chemistry Research* **2014,** 53, (10), 3950-3958.
6. Medina-Herrera, N.; Jiménez-Gutiérrez, A.; Grossmann, I. E., A mathematical programming model

for optimal layout considering quantitative risk analysis. *Computers & Chemical Engineering* **2014,** 68, 165-181.

7. Penteado, F. D.; Ciric, A. R., An MINLP Approach for Safe Process Plant Layout. *Industrial & Engineering Chemistry Research* **1996,** 35, (4), 1354-1361.

8. Lira-Flores, J.; Vázquez-Román, R.; López-Molina, A.; Mannan, M. S., A MINLP approach for layout designs based on the domino hazard index. *Journal of Loss Prevention in the Process Industries* **2014,** 30, 219-227.

9. Alves, D. T. S.; de Medeiros, J. L.; Araújo, O. D. Q. F., Optimal determination of chemical plant layout via minimization of risk to general public using Monte Carlo and Simulated Annealing techniques. *Journal of Loss Prevention in the Process Industries* **2016,** 41, 202-214.

10. Latifi, S. E.; Mohammadi, E.; Khakzad, N., Process plant layout optimization with uncertainty and considering risk. *Computers & Chemical Engineering* **2017,** 106, 224-242.

11. Lee, D. H.; Lee, C. J., The Plant Layout Optimization Considering the Operating Conditions. *Journal of Chemical Engineering of Japan* **2017,** 50, (7), 568-576.

12. Xu, Y.; Wang, Z.; Zhu, Q., An Improved Hybrid Genetic Algorithm for Chemical Plant Layout Optimization with Novel Non-overlapping and Toxic Gas Dispersion Constraints. *Chinese Journal of Chemical Engineering* **2013,** 21, (4), 412-419.

13. Baker, J. A.; Bowman, F. L.; Erwin, G.; Gorton, S.; Hendershot, D.; Leveson, N.; Priest, S.; Rosenthal, I.; Tebo, P. V.; Wiegmann, D. A.; Wilson, L. D. *The report of the BP U.S. refineries independent safety review panel*; 2007.

14. Martinez-Gomez, J.; Nápoles-Rivera, F.; Ponce-Ortega, J. M.; Serna-González, M.; El-Halwagi, M. M., Optimization of facility location and reallocation in an industrial plant through a multi-annual framework accounting for economic and safety issues. *Journal of Loss Prevention in the Process Industries* **2015,** 33, 129-139.

15. Patsiatzis, D. I.; Knight, G.; Papageorgiou, L. G., An MILP approach to safe process plant layout. *Chemical Engineering Research and Design* **2004,** A5, (82), 579 – 586.

16. Jung, S.; Ng, D.; Diaz-Ovalle, C.; Vazquez-Roman, R.; Mannan, M. S., New Approach To Optimizing the Facility Siting and Layout for Fire and Explosion Scenarios. *Industrial & Engineering Chemistry Research* **2011,** 50, (7), 3928-3937.

17. Alnouri, S. Y.; Linke, P.; El-Halwagi, M., Water integration in industrial zones: a spatial representation with direct recycle applications. *Clean Technologies and Environmental Policy* **2014,** 16, (8), 1637-1659.

18. Alnouri, S. Y.; Linke, P.; El-Halwagi, M. M., Synthesis of industrial park water reuse networks considering treatment systems and merged connectivity options. *Computers & Chemical Engineering* **2016,** 91, 289-306.

19. Guirardello, R.; Swaney, R. E., Optimization of process plant layout with pipe routing. *Computers & Chemical Engineering* **2005,** 30, (1), 99-114.

20. Wu, Y.; Wang, Y., A Chemical Industry Area-wide Layout Design Methodology for Piping Implementation. *Chemical Engineering Research & Design* **2017,** 118, 81-93.

21. Chu, C.; Wong, Y., FLUTE: Fast lookup table based rectilinear steiner minimal tree algorithm for VLSI design. *IEEE Transactions on Computer-Aided Design of Integrated Circuits and Systems* **2008,** 27, (1), 70-83.

22. Warme, D. M. Spanning Trees in Hypergraphs with Applicationss to Steiner Trees. University of Virginia, 1998.

23. Griffith, J.; Robins, G.; Salowe, J. S.; Zhang, T., Closing the gap: near-optimal steiner trees in polynomial time. *IEEE Transactions on Computer-Aided Design of Integrated Circuits and Systems* **1994,** 13, (11), 1351-1365.
24. Wu, Y.; Zhang, S.; Wang, Y.; Feng, X., The optimization of area-wide plant layout with piecewise steam pipeline network using parallel genetic algorithm based on GeoSteiner. In *International conference on sustainable energy & environmental protection*, Paisley, UK, 2018.
25. Wang, R.; Wu, Y.; Wang, Y.; Feng, X.; Liu, M., An Industrial Park Layout Design Method Considering Pipeline Length Based on FLUTE Algorithm. In *Computer Aided Chemical Engineering*, Eden, M. R.; Ierapetritou, M. G.; Towler, G. P., ^Eds. Elsevier: 2018; Vol. 44, pp 193-198.
26. Vázquez-Román, R.; Lee, J.; Jung, S.; Mannan, M. S., Optimal facility layout under toxic release in process facilities: A stochastic approach. *Computers & Chemical Engineering* **2010,** 34, (1), 122-133.
27. Caputo, A. C.; Pelagagge, P. M.; Palumbo, M.; Salini, P., Safety-based process plant layout using genetic algorithm. *Journal of Loss Prevention in the Process Industries* **2015,** 34, 139-150.
28. Xie, W.; Sahinidis, N. V., A branch-and-bound algorithm for the continuous facility layout problem. *Computers & Chemical Engineering* **2008,** 32, (4-5), 1016-1028.
29. Wang, R.; Zhao, H.; Wu, Y.; Wang, Y.; Feng, X.; Liu, M., An industrial facility layout design method considering energy saving based on surplus rectangle fill algorithm. *Energy* **2018,** 158, 1038-1051.
30. Lees, F. P., *Loss Prevention in the Process Industries: Hazard Identification, Assessment and Control*. Butterworth-Heinemann Publisher: Oxford, 2001.
31. Brazil, M.; Zachariasen, M., *Optimal Interconnection Trees in the Plane*. Springer International Publishing: Switzerland, 2015.
32. Hanan, M., On Steiner's Problem with Rectilinear Distance. *SIAM Journal on Applied Mathematics* **2006,** 14, (2), 255-265.
33. Chu, C. In *FLUTE: Fast lookup table based wirelength estimation technique*, International Conference on Computer-Aided Design, Digest of Technical Papers, San Jose, CA, United states, 2004; Institute of Electrical and Electronics Engineers Inc.: pp 696-701.
34. Chu, C.; Wong, Y. In *Fast and accurate rectilinear Steiner minimal tree algorithm for VLSI design*, Proceedings of the International Symposium on Physical Design, San Francisco, CA, United states, 2005; Association for Computing Machinery: pp 28-35.
35. Wong, Y.; Chu, C. In *A scalable and accurate rectilinear steiner minimal tree algorithm*, 2008 International Symposium on VLSI Design, Automation, and Test, Hsinchu, Taiwan, 2008; IEEE Computer Society: pp 29-34.
36. Chu, C., FLUTE: Fast Lookup Table Based Technique for RSMT Construction and Wirelength Estimation, 2011, http://home.eng.iastate.edu/~cnchu/flute.htm, Access on: March 9, 2020.
37. Wu, Y.; Wang, R.; Wang, Y.; Feng, X., An area-wide layout design method considering piecewise steam piping and energy loss. *Chemical Engineering Research and Design* **2018,** 138, 405-417.
38. Stijepovic, M. Z.; Linke, P., Optimal waste heat recovery and reuse in industrial zones. *Energy* **2011,** 36, (7), 4019-4031.
39. Wang, Z., *Handbook of Petrochemical Engineering Design Vol.4*. Chemical Industrial Press: China, Beijing, 2015; p 301-303.

Appendix

Proposition: The connection pattern with the lowest cost is contained in the database of the original FLUTE algorithm

According to the length vector, a feasible connection pattern can be determined to be either a potentially optimal connection pattern or a connection pattern that cannot be the shortest, as shown in Figure A1. The original proposition is that the connection pattern with the lowest cost is contained in the database. Therefore, the original proposition can be identified to be true, if a derivative proposition can be proved that any connection pattern that cannot be the shortest also cannot be the most economical one. The derivative proposition is proved in the following.

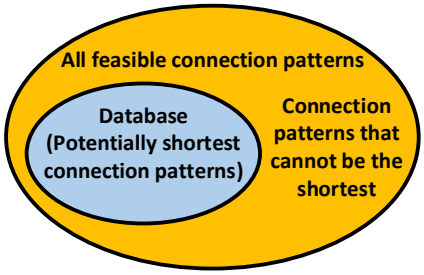

Figure A1 Classification of connection patterns

If a length vector is found that it cannot be the shortest by comparing length vectors, it must have been compared with a potentially optimal length vector. Next, it is going to prove that the cost of a length vector that cannot be the shortest must be higher than the corresponding potentially optimal length vector.

Without loss of generality, it is assumed that p_{no} is a length vector that cannot be the shortest, and p_{po} is the corresponding potentially optimal length vector. p_{no} must have at least one additional pipe segment than p_{po}. Assuming that the additional pipe segments appears in s_i, the sum of mass flow rates in s_i segment of p_{no} must be equal to the sum of p_{po}'s according to a mass balance between the nodes in the left and right part of the network. Assume that the sum of mass flow rates in s_i segment is q_1 in p_{po}, for example, as shown in Figure A2 (a). For p_{no}, the additional pipe segment in s_i will either shunt the mass flow rate of q_1, as shown in Figure A2 (b), or increase the mass flow rate of q_1 with a reverse flow direction, as shown in Figure A2 (c).

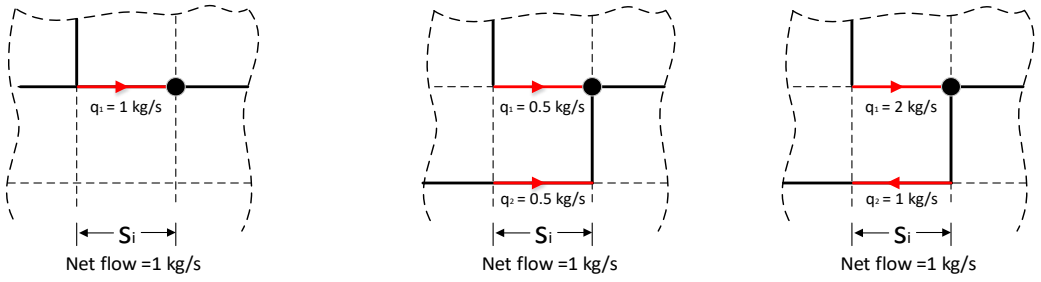

(a) (b) (c)

Figure A2 An illustration of proving

No matter which situation p_{no} is under, p_{no} is more expensive than p_{po}. For the former situation of

shunting, the problem is converted to determine which one is more economical between a thick pipe and two thin pipes with the same total cross section areas. A thick pipe is certainly more economical. For the later situation of reverse direction flow, one of the pipes in p_{no} is thicker, and there is one more pipe. Therefore, p_{no} is more expensive compared with p_{po}. Consequently, the cost of any length vector that cannot be the shortest must be higher than the corresponding potentially optimal length vector.

Now the original proposition is proved that the connection pattern with the lowest cost is still contained in the potentially optimal length vector database.